

# Robust Interference Management for SISO Systems with Multiple Over-the-Air Computations

Jaber Kakar\*, *Student Member, IEEE* and Aydin Sezgin\*, *Senior Member, IEEE*

\*Institute of Digital Communication Systems, Ruhr-Universität Bochum, Germany

Email: {jaber.kakar, aydin.sezgin}@rub.de

## Abstract

Over-the-air computation (AirComp) represents a promising concept that leverages on the superposition property of wireless multiple access channels (MAC). This property facilitates the computation of sums  $s = \sum_{k=1}^K x_k$  of real-valued, distributed sensor (Tx) data  $x_k$  for a fusion center (Rx). In today's context, where spectrum is scarce, we may wish to not only compute one, but rather (for any mutually exclusive collection of sensor index sensor sets  $\mathcal{D}_m$ )  $M$ ,  $M \geq 2$ , sums  $s_m = \sum_{k \in \mathcal{D}_m} x_k$  over a shared complex-valued MAC at once with minimal mean-squared error (MSE). Finding appropriate Tx-Rx scaling factors balance between a low error in the computation of  $s_n$  and the interference induced by it in the computation of other sums  $s_m$ ,  $m \neq n$ . In this paper, we are interested in designing an optimal Tx-Rx scaling policy that minimizes the mean-squared error  $\max_{m \in [1:M]} \text{MSE}_m$  subject to a Tx power constraint with maximum power  $P$ . We show that an optimal design of the Tx-Rx scaling policy  $(\bar{\mathbf{a}}, \bar{\mathbf{b}})$  involves optimizing (a) their phases and (b) their absolute values in order to (i) decompose the computation of  $M$  sums into, respectively,  $M_R$  and  $M_I$  ( $M = M_R + M_I$ ) calculations over real and imaginary part of the Rx signal and (ii) to minimize the computation over each part – real and imaginary – individually. The primary focus of this paper is on (b). We derive conditions (i) on the feasibility of the optimization problem and (ii) on the Tx-Rx scaling policy of a local minimum for  $M_w = 2$  computations over the real ( $w = R$ ) or the imaginary ( $w = I$ ) part. Extensive simulations over one receiving chain for  $M_w = 2$  show that the level of interference in terms of  $\Delta D = |\mathcal{D}_2| - |\mathcal{D}_1|$  plays an important role on the ergodic worst-case MSE. At very high SNR, typically only the sensor with the weakest channel transmits with full power while all remaining sensors transmit with less to limit the interference. Interestingly, we observe that due to residual interference, the ergodic worst-case MSE is not vanishing; rather, it converges to  $\frac{|\mathcal{D}_1||\mathcal{D}_2|}{K}$  as  $\text{SNR} \rightarrow \infty$ .

## Index Terms

Wireless sensor networks, over-the-air computation, mean-squared error, power control

### I. INTRODUCTION

In the era of Big Data and Internet-of-Things (IoT), enormous quantities of data are exchanged among a staggering number of mobile devices (e.g., sensors). According to DOMO, the global internet population grew by 500 million from 2017 to 2018 and reached now 4.3 billions [1] creating around 1.7 MB of data per second. Simultaneously, the number of IoT devices is exponentially growing and forecasts predict 125 billion IoT devices by 2030 [2]. These devices are a key contributing factor in the massive growth of data.

In IoT applications involving massive amount of data, wireless data aggregation (WDA) represents a promising solution for data collection from sensors with limited spectrum bandwidth [3]. WDA is of particular relevance when there are latency restrictions on the processing of sensor data. In AirComp – a novel WDA technique that leverages on the superposition property of the wireless multiple access channel (MAC) – data signals can be combined in both a linear and non-linear manner. Specifically, a fusion center (FC) receives a linear combination of sensor signals weighted by the channels' coefficients. This allows realizing the summation, or averaging, of sensor signals through over-the-air transmissions. Through appropriate pre-processing functions  $\psi_k(\cdot)$  at sensor  $k = 1, \dots, K$ , and post-scaling function  $\varphi(\cdot)$  at the FC not only averaging but more complex target functions  $\phi(\cdot)$  on the sensor data  $(x_1, \dots, x_K)$  from the class of so-called *nomographic functions* (e.g., geometric mean) which omit the representation

$$\phi(x_1, \dots, x_K) = \varphi\left(\sum_{k=1}^K \psi_k(x_k)\right)$$

can be attained [4]. For AirComp systems, the idea in [5]–[7] is to let each sensor process its own data  $x_k$  according to  $\psi_k(x_k)$ , such that the MAC generates the intermediate result  $\sum_{k=1}^K \psi_k(x_k)$  as an input of  $\varphi(\cdot)$  which in return gives the desired function  $\phi$  evaluated on the sensor data  $(x_1, \dots, x_K)$ .<sup>1</sup> The advantage of the decomposition principle in AirComp is

<sup>1</sup>We emphasize that the idea of over-the-air computation has also been applied very early by the information theory community in the construction of the so-called compute-and-forward relaying strategy that harnesses from the interference caused by the simultaneous transmission in a MAC [8].

two-fold. On the one hand, the computation task is decomposed into  $K + 1$  subtasks which are, respectively,  $\psi_k(\cdot)$ ,  $k = 1, \dots, K$ , assigned to the  $k$ -th sensor and  $\varphi(\cdot)$  allotted to the FC. On the other hand, completing the computation is limited to a single time slot rather than a  $K$  slot TDMA scheme. Specific use cases of AirComp are, amongst others, distributed machine learning [9], [10] and over-the air consensus [11].

#### A. Related Work

An important aspect of AirComp research is about its system design. More detailed, the design of pre- and postprocessing functions for different functions  $\phi(\cdot)$  (e.g., geometric mean, maximum) have been analyzed in references [3], [6], [7]. Robust designs that account for synchronization offsets between sensors [7], [12] and imperfect or lack of channel state information [13], [14] are also studied. More recently, two research groups [15], [16] have independently developed for an averaging target function, the jointly global-optimal pre- and postprocessing scalars that minimize the (non-convex) mean-squared error (MSE) subject to a per-sensor, peak transmit power constraint. The authors make the observation that the optimal pre-processing is a mixture of the channel-inversion and energy-greedy policy. In [17], *Zhu et al.* consider the optimization problem that minimizes the computation distortion of a MIMO AirComp system with multi-modal sensors by zero-forcing precoding and aggregation beamforming design. This setup facilitates a multiplexing gain in the sense that at most  $\min(N_T, N_R)^2$  functions  $\phi_m$  can be computed in a single slot. The system model of [17] is extended in [18] to a wirelessly-powered, MIMO AirComp system.

To the best of the authors' knowledge, the aspect of interference management in AirComp systems – particularly for SISO systems with no multiplexing gain – is largely unstudied. As part of this study, the goal is (i) to better understand how multiple computations over a shared MAC influence the computation distortion and (ii) deduce an interference management policy for low, medium and high SNR which minimizes the worst MSE.

#### B. Contributions

In this paper, we consider a single-antenna AirComp system with which we seek to compute, for any mutually exclusive collection of sensor index sensor sets  $\mathcal{D}_m$  of arbitrary

<sup>2</sup> $N_T$  and  $N_R$  are, respectively, the number of transmit (sensor) and receive (FC) antennas.

cardinality,  $M$  sums  $s_m = \sum_{k \in \mathcal{D}_m} x_k$ ,  $m = 1, \dots, M$ , with real-valued sensor inputs  $x_k$  over a shared MAC. As opposed to a MIMO system considered in [17], where there is a multiplexing gain, for a SISO system there is none. For this system under study, the main contributions of this paper are the following.

- We cast the AirComp problem as an optimization problem that minimizes the worst-case MSE –  $\max_{m \in [1:M]} \text{MSE}_m$  – over all possible transmit-receive scaling (Tx-Rx) policies. In this optimization problem, the per-sensor pre-scaling policy is subjected to a power constraint. Due to the coupling of Tx and Rx-scaling, this problem is non-convex.
- An orthogonalization principle that decomposes the computation of  $M$  sums into  $M_R$  computations over the real and  $M_I$  computations over the imaginary part of the receiving chain is suggested ( $M = M_R + M_I$ ). Not only for the special case, where  $M = 2$ , but also larger  $M > 2$ , we show the optimality of this decomposition rule. When this orthogonalization principle is applied, the optimization of the worst-case MSE is separated for real and imaginary part.
- The worst-case MSE optimization along one part – say without loss of generality the real part – for  $M_R = 2$  computations is considered. For this case, the MSE minimization problem is reformulated to a fractional program. We study its feasibility and derive conditions on the maximum tolerable noise variance. Through means of the Karush-Kuhn-Tucker (KKT) condition [19], we determine a close-form expression which satisfies the second-order sufficient condition of relative matrix inertias [20] of local minima. The solution resembles global optimal solutions of interference-free scenarios [15], [16] in the sense that sensors  $k \in \mathcal{P}_m \subseteq \mathcal{D}_m$ ,  $m \in [1 : M_R]$ , with stronger channels transmit with less-than full power while all remaining sensors operate at peak power. The cardinality of these sets are of utmost importance for optimal interference management.
- We consider in our simulations a single receiving chain – say without loss of generality the real part – for  $M_R = 2$  computations.<sup>3</sup> They show that the level of interference in terms of  $\Delta \mathcal{D} = |\mathcal{D}_2| - |\mathcal{D}_1|$  plays an important role on the ergodic worst-case MSE. At very high SNR, typically only the sensor with the weakest channel transmits with full power while all remaining sensors transmit with less to limit the interference. Interestingly, we observe that due to residual interference, the ergodic worst-case MSE is not vanishing;

<sup>3</sup>In the simulations,  $K = |\mathcal{D}_1| + |\mathcal{D}_2|$  holds.

rather, it converges to  $\frac{|\mathcal{D}_1||\mathcal{D}_2|}{K}$  as  $\text{SNR} \rightarrow \infty$ . This result gives us an approximate design guideline on deciding which pair of computation indices  $(m_{1,w}, m_{2,w})$  shall be computed along the real ( $w = R$ ) and imaginary ( $w = I$ ) processing chain.

### C. Paper Organization

The remainder of this paper is organized as follows. Section II deals with the AirComp system model and its respective MSE optimization problem. In section III, the orthogonalization principle for multiplexing the real-valued computation along real and imaginary part of the receiving chain is described. The optimization problem after orthogonalization is formulated and solved in the section IV. The main subject of section V is the discussion of the simulation results. Finally, section VI concludes this work.

**Notations:** For a complex number  $z$ ,  $\Re\{z\}$  and  $\Im\{z\}$  denote, respectively, the real and imaginary part.  $z^*$  is the complex conjugate of  $z$ . Throughout this paper, we denote sets by calligraphic letters (e.g.,  $\mathcal{S}$ ), vectors by bold, lower-case letters (e.g.,  $\mathbf{b}$ ) and matrices by capitalized, bold-face letters (e.g.,  $\mathbf{B}$ ).  $\mathbf{x}_{[i]}$  represents the  $i$ -th largest component in  $\mathbf{x}$  and  $\mathbf{x}_{\mathcal{S}}$  is the collection of elements of  $\mathbf{x} = (x_1, x_2, \dots, x_N)^T$  indexed by  $\mathcal{S} \subseteq [1 : N]$ .  $\text{sign}\{x\}$  is the signum function that extracts the sign of a real number  $x$ . Finally, we use  $[x]^+$  as a shorthand notation for  $\max(0, x)$ .

## II. SYSTEM MODEL AND PROBLEM FORMULATION

### A. System Model

We consider a  $K$ -sensor, single-antenna AirComp multiple access channel (MAC) system as shown in Fig. 1. In this system, each sensor's pre-processed signal  $x_k \in \mathbb{R}$ ,  $\forall k \in [1 : K]$ , is scaled by its scaling factor  $\bar{b}_k \in \mathbb{C}$  and conveyed to the receiver (FC) through the MAC. The collection of all  $K$  Tx-scaling factors are denoted by  $\bar{\mathbf{b}} \triangleq (\bar{b}_k)_{k \in [1:K]}$ . Thus, the received signal  $y$  becomes

$$y = \sum_{k=1}^K \bar{h}_k \bar{b}_k x_k + n, \quad (1)$$

where  $h_k \in \mathbb{C}$  is the channel coefficient of sensor  $k$  and  $n \sim \mathcal{CN}(0, 2\sigma^2)$  is additive white Gaussian noise. We assume that the channel coefficients  $\bar{\mathbf{h}} \triangleq (\bar{h}_k)_{k \in [1:K]}$  are both known by the sensors and the receiver. Additionally, the sensors transmissions are assumed to be

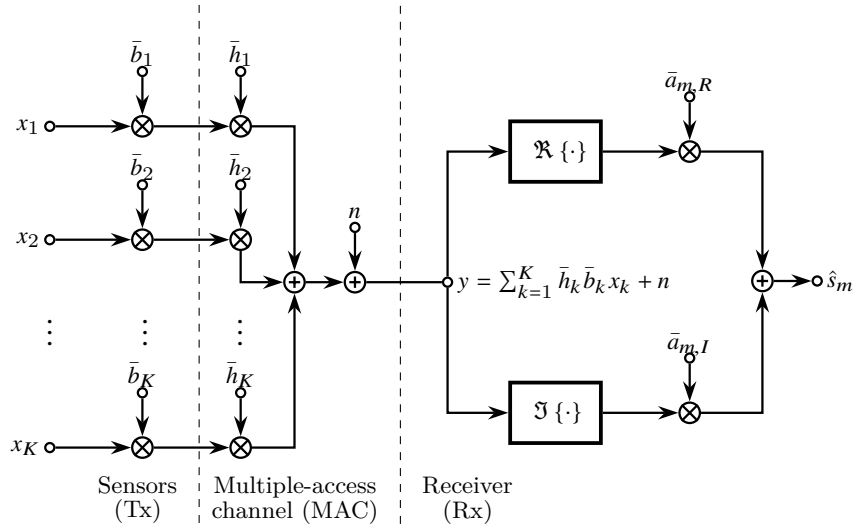


Fig. 1: Illustration of the AirComp system. Note that  $x_k$ ,  $\bar{a}_{m,R}$ ,  $\bar{a}_{m,I}$  and  $\hat{s}_m$  are real, while the remaining variables are typically complex.

perfectly synchronized. The pre-processed sensor signals  $x_k$ ,  $\forall k \in [1 : K]$ , are independent of each other with each of them being zero mean and unit variance.

Under these assumptions, the goal of the AirComp problem with *multiple simultaneous computations* is to compute  $M$ ,  $M \geq 2$ , desired sums  $(s_m)_{m \in [1:M]}$  given by

$$s_m = \sum_{k \in \mathcal{D}_m} x_k \quad (2)$$

over the MAC at once with the lowest possible computation distortion. The indexing sets  $\mathcal{D}_m$ <sup>4</sup> denote which sensors collaborate in the computation of the  $m$ -th sum  $s_m$ . We do not make any assumptions on the realizations of  $\mathcal{D}_m$  other than  $\mathcal{D}_m \neq \emptyset$ , and  $\mathcal{D}_m \cap \mathcal{D}_n = \emptyset$ ,  $m \neq n$ ,  $\forall m, n \in [1 : M]$ .

The computation distortion is measured by the mean-squared error (MSE)

$$\text{MSE}_m = \mathbb{E} [|\hat{s}_m - s_m|^2], \quad (3)$$

where  $\hat{s}_m$  is a linear estimate of  $s_m$  given by

$$\hat{s}_m = \bar{a}_{m,R} \Re \{y\} + \bar{a}_{m,I} \Im \{y\} = \Re \{\bar{a}_{m,R}^* y\} \quad (4)$$

<sup>4</sup>We call  $\mathcal{D}_m$  the  $m$ -th *computation sensor* index set.

with  $\bar{a}_m^*$  being the complex conjugate of the  $m$ -th Rx-scaling factor  $\bar{a}_m = \bar{a}_{m,R} + j\bar{a}_{m,I} \in \mathbb{C}$  of the vector  $\bar{\mathbf{a}} \triangleq (\bar{a}_m)_{m \in [1:M]}$ . By the assumption that  $x_k$  is of zero mean and unit variance, the power consumption of sensor  $k$  is  $\mathbb{E}[|\bar{b}_k x_k|^2] = |\bar{b}_k|^2$ . In the remainder of this paper, we denote the absolute values of  $\bar{b}_k$  and  $\bar{h}_k$  by  $b_k$  and  $h_k$ , respectively.

### B. Problem Formulation

A more explicit representation of  $\text{MSE}_m$  as a function of  $\bar{\mathbf{a}}$  and  $\bar{\mathbf{b}}$  using  $\tilde{b}_k = \bar{h}_k \bar{b}_k$  is

$$\text{MSE}_m = \sum_{k \in \mathcal{D}_m} |\Re\{\bar{a}_m^* \tilde{b}_k\} - 1|^2 + \sum_{\ell \in \mathcal{D}_m^C} |\Re\{\bar{a}_m^* \tilde{b}_\ell\}|^2 + \sigma^2 |\bar{a}_m|^2, \quad (5)$$

where  $\mathcal{D}_m^C \triangleq [1 : K] \setminus \mathcal{D}_m$ . Alternatively, we may rewrite (5) in its polar form using  $\phi_k = \arg\{\tilde{b}_k\}$  and  $\alpha_m = \arg\{\bar{a}_m\}$ .

$$\begin{aligned} \text{MSE}_m = & \sum_{k \in \mathcal{D}_m} \left| |\bar{a}_m \tilde{b}_k| \cos(\phi_k - \alpha_m) - 1 \right|^2 \\ & + \sum_{\ell \in \mathcal{D}_m^C} \left| |\bar{a}_m \tilde{b}_\ell| \cos(\phi_\ell - \alpha_m) \right|^2 + \sigma^2 |\bar{a}_m|^2 \end{aligned} \quad (6)$$

Now, for given channel realizations  $\bar{\mathbf{h}}$ , a *robust* MSE-minimization problem in terms of a combined Tx-Rx policy, i.e., designing  $(\bar{\mathbf{a}}, \bar{\mathbf{b}})$  *jointly*, can be formulated according to

$$\min_{\bar{\mathbf{a}}, \bar{\mathbf{b}}} \max_{m \in [1:M]} \text{MSE}_m \quad (7a)$$

$$\text{subject to } b_k^2 \leq P, \forall k \in [1 : K]. \quad (7b)$$

### III. ORTHOGONALIZATION OVER REAL AND IMAGINARY PARTS

From Eq. (5) one can infer that when optimizing an individual MSE, say  $\text{MSE}_m$ , it is preferable to choose for  $|\bar{a}_m \tilde{b}_k| \neq 0, \forall k \in [1 : K]$

$$\Im\{\bar{a}_m^* \tilde{b}_k\} = 0, \quad \forall k \in \mathcal{D}_m,$$

$$\Re\{\bar{a}_m^* \tilde{b}_\ell\} = 0, \quad \forall \ell \in \mathcal{D}_m^C.$$

In (6) this translates to setting the phase differences to  $\phi_k - \alpha_m = 0, \phi_\ell - \alpha_m = \pm\pi/2, \forall k \in \mathcal{D}_m, \forall \ell \in \mathcal{D}_m^C$ . As a result,  $\text{MSE}_m$  is interference-free and corresponds to the point-to-point MSE, denoted by  $\text{MSE}_m^{(\text{P2P})}$ <sup>5</sup>

$$\text{MSE}_m^{(\text{P2P})} = \sum_{k \in \mathcal{D}_m} \left| |\bar{a}_m \tilde{b}_k| - 1 \right|^2 + \sigma^2 |\bar{a}_m|^2, \quad (8)$$

<sup>5</sup>The optimization of  $\text{MSE}_m^{(\text{P2P})}$  with respect to parameters  $a_m$  and  $b_k, k \in \mathcal{D}_m$  is discussed in detail in [15], [16].

while the remaining MSEs –  $\text{MSE}_n, \forall n \in [1 : M], n \neq m$  – equal

$$\begin{aligned} \text{MSE}_n &= \sum_{k \in \mathcal{D}_n} \left| |\bar{a}_n \tilde{b}_k| \cos \left( \alpha_m - \alpha_n \pm \frac{\pi}{2} \right) - 1 \right|^2 + \sum_{\ell \in \mathcal{D}_m} \left| |\bar{a}_n \tilde{b}_\ell| \cos (\alpha_m - \alpha_n) \right|^2 \\ &+ \sum_{\ell \in \mathcal{D}_n^c \setminus \mathcal{D}_m} \left| |\bar{a}_n \tilde{b}_\ell| \cos \left( \alpha_m - \alpha_n \pm \frac{\pi}{2} \right) \right|^2 + \sigma^2 |\bar{a}_n|^2. \end{aligned} \quad (9)$$

For the special case  $M = 2$ , where  $\mathcal{D}_n^c \setminus \mathcal{D}_m = \emptyset$ , it is *optimal* to choose  $\alpha_m - \alpha_n = \mp \pi/2$  in (9) such that  $\text{MSE}_n = \text{MSE}_n^{\text{(P2P)}}$ . For this special case, a simple choice that satisfies all phase difference conditions is  $(\alpha_m, \alpha_n) = (\phi_k, \phi_\ell) = (0, \pi/2) \forall k \in \mathcal{D}_m, \forall \ell \in \mathcal{D}_n, m \neq n$ . Simply said, this strategy *orthogonalizes* the computation of  $s_1$  and  $s_2$ , i.e.,  $s_m$  is either solely computed along the real ( $\bar{a}_{m,I} = 0$ ) or imaginary ( $\bar{a}_{m,R} = 0$ ) Rx processing chain of Fig. 1.

We can extend this orthogonalization strategy to the case where  $M > 2$ . To this end, we define real and imaginary *computation index* sets  $\mathcal{C}_R \subseteq [1 : M]$  and  $\mathcal{C}_I \subseteq [1 : M]$ ,  $\mathcal{C}_R \cup \mathcal{C}_I = [1 : M]$ , that assign which computation is delegated to real and imaginary processing chains. The union  $\mathcal{C}_R \cap \mathcal{C}_I$ <sup>6</sup> specifies the computations that are computed along both chains. In this paper, we assume that  $\mathcal{C}_R \cap \mathcal{C}_I = \emptyset$  such that  $M = M_R + M_I$ . Then, for a given computation index set pair  $(\mathcal{C}_R, \mathcal{C}_I)$

$$\begin{aligned} \text{MSE}_{m,w}^\perp(\mathcal{C}_w) &= \sum_{k \in \mathcal{D}_m} \left| |\bar{a}_{m,w}| h_k b_k - 1 \right|^2 \\ &+ \sum_{\ell \in \mathcal{D}_{\mathcal{C}_w} \setminus \mathcal{D}_m} \left| |\bar{a}_{m,w}| h_\ell b_\ell \right|^2 + \sigma^2 |\bar{a}_{m,w}|^2, \end{aligned} \quad (10)$$

$$\text{MSE}_w^\perp(\mathcal{C}_w) = \min_{\substack{(|\bar{a}_{m,w}|)_{m \in \mathcal{C}_w}, \\ (b_k)_{k \in \mathcal{D}_{\mathcal{C}_w}} \leq \sqrt{P} \mathbf{1}}} \max_{m \in \mathcal{C}_w} \left( \text{MSE}_{m,\mathcal{C}_w}^\perp \right), \quad (11)$$

denote, respectively, the associated MSE of  $s_m$  and the optimized, worst-case MSE of all computations along Rx processing chain  $w \in \{R, I\}$ . Overall, the worst-case MSE for this pair then becomes

$$\text{MSE}^\perp(\mathcal{C}_R, \mathcal{C}_I) = \max \left( \text{MSE}_R^\perp(\mathcal{C}_R), \text{MSE}_I^\perp(\mathcal{C}_I) \right). \quad (12)$$

Note that *symmetry* applies, i.e., processing computations with indices in  $\mathcal{C}_R$  ( $\mathcal{C}_I$ ) can be processed either along the real and imaginary Rx processing chain; thus,  $\text{MSE}_w^\perp(\mathcal{C}_w) =$

<sup>6</sup>We denote the cardinalities by  $M_w = |\mathcal{C}_w|, w \in \{R, I\}$ . Note that these cardinalities in its most general form satisfy  $M \leq M_R + M_I$ .



$\text{MSE}_{\bar{w}}^{\perp}(\mathbf{C}_w)$  for  $w \neq \bar{w}$ . Solving (12) over all possible pairs  $(\mathbf{C}_R, \mathbf{C}_I)$  gives the optimal MSE of the orthogonalization scheme.

$$\text{MSE}^{\perp\star} \triangleq \text{MSE}^{\perp}(\mathbf{C}_R^{\star}, \mathbf{C}_I^{\star}) = \min_{\substack{(\mathbf{C}_R^{\star}, \mathbf{C}_I^{\star}) \in \mathbb{N}_{++}^2 \\ \mathbf{C}_R \cup \mathbf{C}_I = [1:M]}} \text{MSE}^{\perp}(\mathbf{C}_R, \mathbf{C}_I) \quad (13)$$

In general,  $\text{MSE}^{\perp\star} \geq \text{MSE}^{\star}$ , with  $\text{MSE}^{\star}$  being the optimum of problem (7). In fact, in Appendix A, we show that equality holds. The basic operation needed to perform the optimization in (12) and (13) is solving (11). To this end, the next section addresses the solution of (11) for the special case of  $M_w = 2$ .

#### IV. SOLUTION TO OPTIMIZATION PROBLEM (11)

In this section, we outline the main ideas and concepts of our locally optimal solution to problem (11). Rigorous proofs are appended to the appendix and referred to wherever necessary.

##### A. Preliminaries

Due to the symmetry property, we consider without loss of generality the optimization problem (11) for the real Rx processing chain when  $M_R = 2$ . In the sequel of this paper, for ease of presentation, we simplify some notation<sup>7</sup>. With this simplification in notation,  $\text{MSE}_{m, \mathbf{C}_R}^{\perp}$  becomes

$$\text{MSE}_m(c_m, \mathbf{b}) = c_m^2 \underbrace{\left( \sigma^2 + \sum_{k=1}^K h_k^2 b_k^2 \right)}_{\triangleq A} - 2c_m \underbrace{\left( \sum_{k \in \mathcal{D}_m} h_k b_k \right)}_{\triangleq B_{\mathcal{D}_m}} + |\mathcal{D}_m|. \quad (14)$$

Note that  $A = \sigma^2 + \sum_{k=1}^K h_k^2 b_k^2 = \sigma^2 + \sum_{m=1}^2 C_{\mathcal{D}_m}$ , where  $C_{\mathcal{D}_m} = \sum_{k \in \mathcal{D}_m} h_k^2 b_k^2$ . From the Cauchy-Schwarz inequality and  $A \geq C_{\mathcal{D}_m}$ , we know that  $B_{\mathcal{D}_m}^2/A \leq B_{\mathcal{D}_m}^2/C_{\mathcal{D}_m} \leq |\mathcal{D}_m|$  and thus  $A|\mathcal{D}_m| - B_{\mathcal{D}_m}^2 \geq 0$ . The comparison of the different MSEs for non-negative Rx-scaling factors

<sup>7</sup>We denote  $|\bar{a}_{m,R}| = c_m$  and pretend that  $\mathbf{C}_I = \emptyset$  such that  $\cup_{m=1}^2 \mathcal{D}_m = [1 : K]$  for  $\mathbf{C}_R = [1 : M] = \{1, 2\}$ . We implicitly assume in this section that  $b_k$ ,  $c_m$  and  $h_k$  are non-negative. Throughout the remaining part of this paper, we omit using the subscript 'R' and the superscript ' $\perp$ '.

$c_m$  in Appendix B allows us to reformulate the optimization problem (11) to the following fractional program for  $\Delta D \triangleq |\mathcal{D}_2| - |\mathcal{D}_1|$ .

$$\min_{\mathbf{b} \geq \mathbf{0}} \quad -\frac{B_{\mathcal{D}_1}^2}{A} \quad (15a)$$

$$\text{subject to } b_k - \sqrt{P} \leq 0, \forall k \in [1 : K], \quad (15b)$$

$$\frac{B_{\mathcal{D}_1}^2 - B_{\mathcal{D}_2}^2}{A} + \Delta D = 0. \quad (15c)$$

Throughout this paper, we denote, respectively, the  $k$ -th *inequality* constraint function by  $g_k(\mathbf{b}) \triangleq b_k - \sqrt{P}$  and the *equality* constraint function by  $h(\mathbf{b}) = B_{\mathcal{D}_1}^2/A - B_{\mathcal{D}_2}^2/A + \Delta D$ .

### B. Feasibility of Problem (15)

In this subsection, we would like to know when problem (15) is infeasible. Clearly, for  $b_k \in [0, \sqrt{P}]$ ,  $\forall k \in [1 : K]$ , there exists no solution if the equality constraint (15c) is not satisfied. Interestingly, in the case that  $\Delta D = 0$ , the optimization problem is always feasible. This is since (15c) reduces to the linear condition  $B_{\mathcal{D}_2} - B_{\mathcal{D}_1} = 0$  for which there incurs no requirement on the noise variance  $\sigma^2$ ; thus, one can always find a feasible vector  $\mathbf{b}$  satisfying that particular equality constraint. Henceforth, we assume that  $\Delta D \neq 0$ . Then, (15c) is not satisfied for  $\mathbf{0} \leq \mathbf{b} \leq \sqrt{P}\mathbf{1}$  and  $\sigma^2 > 0$  if

$$\sigma^2 > \tilde{\sigma}^2 \triangleq \left[ \max_{\mathbf{0} \leq \mathbf{b} \leq \sqrt{P}\mathbf{1}} \left( \frac{1}{\Delta D} (B_{\mathcal{D}_2}^2 - B_{\mathcal{D}_1}^2) - C_{\mathcal{D}_1} - C_{\mathcal{D}_2} \right) \right]^+. \quad (16)$$

In other words, the problem has no solution if the noise variance  $\sigma^2$  exceeds the threshold noise variance  $\tilde{\sigma}^2$ . This threshold can be further simplified by

$$\tilde{\sigma}^2 = \begin{cases} \left[ \max_{\substack{0 \leq b_k \leq \sqrt{P} \\ k \in \mathcal{D}_2}} \left( \frac{1}{\Delta D} B_{\mathcal{D}_2}^2 - C_{\mathcal{D}_2} \right) \right]^+ & \text{if } \Delta D > 0 \\ \left[ \max_{\substack{0 \leq b_k \leq \sqrt{P} \\ k \in \mathcal{D}_1}} \left( -\frac{1}{\Delta D} B_{\mathcal{D}_1}^2 - C_{\mathcal{D}_1} \right) \right]^+ & \text{if } \Delta D < 0 \end{cases}. \quad (17)$$

1) *Lower Bound  $\tilde{\sigma}^2$* : In the following, we establish a lower bound  $\underline{\tilde{\sigma}}^2$  on  $\tilde{\sigma}^2$ . A lower bound on  $\tilde{\sigma}^2$  is to choose a mixture of full power transmission, i.e.,  $b_k = \sqrt{P}$  for  $k \in \mathcal{G}_i^C \subseteq \mathcal{D}_i$  and less-than full power transmission, i.e.,  $b_j = \frac{H_{\mathcal{G}_i}}{h_j} < \sqrt{P}$  for  $j \in \mathcal{G}_i \subseteq \mathcal{D}_i$ , where  $\mathcal{G}_i \cup \mathcal{G}_i^C = \mathcal{D}_i$ . Specifically, we choose

$$H_{\mathcal{G}_i} = \frac{\sqrt{P} \left( \sum_{k \in \mathcal{G}_i^C} h_k \right)}{(-1)^i \Delta D - |\mathcal{G}_i|}$$

for  $(-1)^j \Delta D - |\mathcal{G}_i| > 0$  such that

$$h_k \sqrt{P} \leq H_{\mathcal{G}_i} \leq h_j \sqrt{P}$$

for  $j \in \mathcal{G}_i$  and  $k \in \mathcal{G}_i^C$ . Above inequality suggests that the indices of the smallest  $|\mathcal{G}_i^C|$  channel coefficients are attributed to the set  $\mathcal{G}_i^C$ . The remaining  $|\mathcal{G}_i|$  indices construct  $\mathcal{G}_i$ .

For this choice of  $b_k$ ,  $k \in \mathcal{D}_i$ , we get

$$\begin{aligned} \underline{\tilde{\sigma}}^2 = & \\ & \left\{ \left[ \frac{1}{\Delta D} \left( |\mathcal{G}_2| H_{\mathcal{G}_2} + \sqrt{P} \left( \sum_{k \in \mathcal{G}_2^C} h_k \right) \right)^2 - \left( |\mathcal{G}_2| H_{\mathcal{G}_2}^2 + P \left( \sum_{k \in \mathcal{G}_2^C} h_k^2 \right) \right) \right]^+ \quad \text{if } \Delta D > 0 \right. \\ & \left. \left[ -\frac{1}{\Delta D} \left( |\mathcal{G}_1| H_{\mathcal{G}_1} + \sqrt{P} \left( \sum_{k \in \mathcal{G}_1^C} h_k \right) \right)^2 - \left( |\mathcal{G}_1| H_{\mathcal{G}_1}^2 + P \left( \sum_{k \in \mathcal{G}_1^C} h_k^2 \right) \right) \right]^+ \quad \text{if } \Delta D < 0 \right. \end{aligned} \quad (18)$$

However, it may often be cumbersome to determine  $H_{\mathcal{G}_i}$ . To this end, we seek to find an upper bound  $\overline{\tilde{\sigma}}^2$  which ultimately allows us to approximate  $\tilde{\sigma}^2$ .

2) *Upper Bound  $\overline{\tilde{\sigma}}^2$* : We can verify that  $B_{\mathcal{D}_m}^2 = C_{\mathcal{D}_m} + F_{\mathcal{D}_m}$ , where

$$F_{\mathcal{D}_m} = \sum_{k \in \mathcal{D}_m} \sum_{\substack{j \in \mathcal{D}_m: \\ j \neq k}} h_k h_j b_k b_j.$$

Since  $\tilde{\sigma}^2$  in (17) depends on both  $C_{\mathcal{D}_i}$  and  $F_{\mathcal{D}_i}$ , we find an upper bound on  $F_{\mathcal{D}_i}$  as a function of  $C_{\mathcal{D}_i}$ .

$$\begin{aligned} F_{\mathcal{D}_i} &= \sum_{k \in \mathcal{D}_i} \sum_{\substack{j \in \mathcal{D}_i: \\ j \neq k}} h_k h_j b_k b_j \stackrel{(a)}{=} \sum_{k \in \mathcal{D}_i} \left( h_k b_k \mathbf{1}_{|\mathcal{D}_i|-1}^T \mathbf{q}_{\mathcal{D}_i \setminus \{k\}} \right) \\ &\stackrel{(b)}{\leq} \sum_{k \in \mathcal{D}_i} \left( \sqrt{|\mathcal{D}_i| - 1} h_k b_k \sqrt{\sum_{j \in \mathcal{D}_i \setminus \{k\}} h_j^2 b_j^2} \right) \\ &\leq \sqrt{|\mathcal{D}_i| - 1} \sqrt{C_{\mathcal{D}_i}} \underbrace{\sum_{k \in \mathcal{D}_i} h_k b_k}_{=B_{\mathcal{D}_i} = \sqrt{C_{\mathcal{D}_i} + F_{\mathcal{D}_i}}} \quad , \end{aligned}$$

where step (a) uses  $\mathbf{q}_{\mathcal{D}_i \setminus \{k\}} = (h_j b_j)_{j \in \mathcal{D}_i \setminus \{k\}}$  such that  $\mathbf{1}_{|\mathcal{D}_i|-1}^T \mathbf{q}_{\mathcal{D}_i \setminus \{k\}} = \sum_{j \in \mathcal{D}_i \setminus \{k\}} h_j b_j$ . Step (b) follows from the Cauchy-Schwarz inequality  $|\mathbf{u}^T \mathbf{v}| \leq \|\mathbf{u}\|_2 \|\mathbf{v}\|_2$  with  $\mathbf{u} = h_k b_k \mathbf{1}_{|\mathcal{D}_i|-1}^T$ ,

$\mathbf{v} = \mathbf{q}_{\mathcal{D}_i \setminus \{k\}}$ ,  $\|\mathbf{u}\|_2 = \sqrt{|\mathcal{D}_i| - 1} h_k b_k$  and  $\|\mathbf{v}\|_2 = \sqrt{\sum_{j \in \mathcal{D}_i \setminus \{k\}} h_j^2 b_j^2} = \sqrt{C_{\mathcal{D}_i} - h_k^2 b_k^2}$ <sup>8</sup>. From  $F_{\mathcal{D}_i} \geq 0$  and above inequality, one can derive that

$$0 \leq F_{\mathcal{D}_i} \leq \frac{C_{\mathcal{D}_i}}{2} \left( |\mathcal{D}_i| - 1 + \underbrace{\sqrt{(|\mathcal{D}_i| - 1)(|\mathcal{D}_i| + 3)}}_{\triangleq \zeta_{\mathcal{D}_i}} \right). \quad (19)$$

Using (19) along with  $C_{\mathcal{D}_i} \leq P \left( \sum_{k \in \mathcal{D}_i} h_k^2 \right)$  in Eq. (17), we get

$$\tilde{\sigma}^2 \triangleq \begin{cases} \frac{P \left( \sum_{k \in \mathcal{D}_2} h_k^2 \right)}{2} \left( \frac{1 - 2\Delta D + |\mathcal{D}_2| + \zeta_{\mathcal{D}_2}}{\Delta D} \right) & \text{if } \Delta D > 0 \\ -\frac{P \left( \sum_{k \in \mathcal{D}_1} h_k^2 \right)}{2} \left( \frac{1 + 2\Delta D + |\mathcal{D}_1| + \zeta_{\mathcal{D}_1}}{\Delta D} \right) & \text{if } \Delta D < 0 \end{cases}. \quad (20)$$

3) *Approximation on  $\tilde{\sigma}^2$* : Since  $\zeta_{\mathcal{D}_i} \approx |\mathcal{D}_i| - 1$ , we approximate  $\tilde{\sigma}^2$  by

$$\tilde{\sigma}^2 \approx \begin{cases} \frac{P |\mathcal{D}_1| \left( \sum_{k \in \mathcal{D}_2} h_k^2 \right)}{\Delta D} & \text{if } \Delta D > 0 \\ \frac{P |\mathcal{D}_2| \left( \sum_{k \in \mathcal{D}_1} h_k^2 \right)}{-\Delta D} & \text{if } \Delta D < 0 \end{cases}.$$

As far as the existence of a feasible solution to the optimization problem is concerned, the approximation on  $\tilde{\sigma}^2$  suggests the following main influencing factors on the non-emptiness of the feasible set. These are (i) the SNR =  $P/\sigma^2$ , (ii) the ratio  $|\mathcal{D}_1|/\Delta D$  ( $|\mathcal{D}_2|/-\Delta D$ ) for  $\Delta D > 0$  ( $\Delta D < 0$ ) and (iii) the channel statistics, i.e., mean and variance of  $h_k$ . As any one of these three factors increases, it is less likely that the feasible set is empty.

### C. Solution through KKT-Conditions

We determine a solution to the optimization problem by considering the KKT-conditions given in Appendix C. The complementary slackness condition (44) suggests that there are two sets of sensors. On the one hand, there are sensors  $k \in \mathcal{P}_m$ ,  $\mathcal{P}_m \subseteq \mathcal{D}_m$ ,  $\forall m \in [1 : 2]$ , that do not transmit with full power, i.e.,  $b_k < \sqrt{P}$ , and thus the Lagrange multiplier being  $\lambda_k = 0$ . The remaining sensors  $\mathcal{P}_m^C = \mathcal{D}_m \setminus \mathcal{P}_m$ ,  $\forall m \in [1 : 2]$ , on the other hand, transmit with full power, i.e.,  $b_k = \sqrt{P}$  for  $k \in \mathcal{P}_m^C$ . In Appendix D, we use these two sets to determine the KKT-point  $\mathbf{b}' = (b'_1, \dots, b'_K)^T$  with its  $k$ -th element being either  $b'_k = \sqrt{P}$  if  $k \in \bigcup_{m=1}^2 \mathcal{P}_m^C$  and  $b'_k = \frac{E_{\mathcal{P}_m}}{h_k}$  if  $k \in \bigcup_{m=1}^2 \mathcal{P}_m$ . We show that the extreme cases where *a*) all sensors transmit with less-than full power, i.e.,  $(|\mathcal{P}_1|, |\mathcal{P}_2|) = (|\mathcal{D}_1|, |\mathcal{D}_2|)$ , and *b*) all sensors transmit with full

<sup>8</sup>In the next step, we use the upper bound  $\sqrt{C_{\mathcal{D}_i} - h_k^2 b_k^2} \leq \sqrt{C_{\mathcal{D}_i}}$  instead of the tighter bound  $\sqrt{C_{\mathcal{D}_i} - h_k^2 b_k^2} \leq \sqrt{C_{\mathcal{D}_i}} \left( 1 - \frac{h_k^2 b_k^2}{2C_{\mathcal{D}_i}} \right)$  for more compact bounding expressions.

power, i.e.,  $(|\mathcal{P}_1|, |\mathcal{P}_2|) = (0, 0)$ , do not give us a feasible KKT-point. Instead, the only viable KKT-solutions occur at intermediate cardinality cases of *a*) and *b*) where  $0 < |\mathcal{P}_1| + |\mathcal{P}_2| < K$  or  $0 < |\mathcal{P}_1^C| + |\mathcal{P}_2^C| < K$ . These give us the cases *c*)  $(|\mathcal{P}_1|, |\mathcal{P}_2|) \geq (1, 1)$  (excluding case *a*)) or *d*)  $|\mathcal{P}_m| \geq 1, |\mathcal{P}_n| = 0, m \neq n$ . For cases *c*) and *d*), we derive conditions on  $E_{\mathcal{P}_m}$  specified in Eqs. (64), (65), such that  $\mathbf{b}'$  and its respective (Lagrange) dual vector  $\boldsymbol{\lambda}' = (\lambda'_1, \dots, \lambda'_K)^T$  produce a KKT-solution that is both primal feasible (cf. Eqs. (41), (42)) and dual feasible (cf. Eq. (43)). Further, from the conditions (64), (65), we can also retrieve the design principle of the sets  $\mathcal{P}_m$  and  $\mathcal{P}_m^C, \forall m \in [1 : 2]$ . That is, for  $m \in [1 : 2]$ , the sensors of the strongest  $|\mathcal{P}_m|$  channels  $h_k$  of the vector  $\mathbf{h}_{\mathcal{D}_m} \triangleq (h_k)_{k \in \mathcal{D}_m}$  are attributed to  $\mathcal{P}_m$ , while the remaining  $|\mathcal{P}_m^C| = |\mathcal{D}_m| - |\mathcal{P}_m|$  sensors with weaker channels in  $\mathbf{h}_{\mathcal{D}_m}$  are accumulated in the set  $\mathcal{P}_m^C$ . Interestingly, this design choice is in agreement with intuition. As one would assume, it is important to exploit every sensors computation to keep the MSE as low as possible. To this end, one seeks to balance out the effective power surplus  $|h_k b_k - h_\ell b_\ell|$  of sensors  $k \in \mathcal{P}_m$  with stronger channels  $h_k$  against sensors  $\ell \in \mathcal{P}_m^C$  with weaker channels  $h_\ell$ . Naturally, the cardinality of  $\mathcal{P}_m$  categorizes the relative level of weak to strong channels and thus plays a crucial role in the achievable worst-case MSE.

#### D. Linear Independence Constraint Qualification (LICQ)

We recall that in order for a minimum point  $\mathbf{b}'$  to satisfy the KKT-conditions of Appendix C, the problem should satisfy some regularity conditions. One common condition, which we use here is the LICQ. The LICQ is satisfied if the gradients of the active inequality constraints, i.e.,  $\nabla g_k(\mathbf{b}'), \forall k \in \bigcup_{m=1}^2 \mathcal{P}_m^C$ , and the gradient of the equality constraint  $\nabla h(\mathbf{b}')$  are linearly independent at  $\mathbf{b}'$ ; or, in other words, the  $K \times (|\mathcal{P}_1^C| + |\mathcal{P}_2^C| + 1)$  matrix

$$\mathbf{J} = \begin{bmatrix} \mathbf{G}(\mathbf{b}') & \nabla h(\mathbf{b}') \end{bmatrix}, \quad (21)$$

where  $\mathbf{G}(\mathbf{b}') = (\nabla g_k(\mathbf{b}'))_{k \in \bigcup_{m=1}^2 \mathcal{P}_m^C}$  has to be of full rank. Thus  $\text{rank}(\mathbf{J}) = |\mathcal{P}_1^C| + |\mathcal{P}_2^C| + 1$ . In Appendix E, we show that the LICQ is satisfied for the KKT-point  $\mathbf{b}'$  of Appendix D.

#### E. Second-Order Sufficient Condition

Consider the Lagrangian function

$$\mathcal{L}(\mathbf{b}, \boldsymbol{\lambda}, \mu) = -\frac{B_{\mathcal{D}_1}^2}{A} + \sum_{k=1}^K \lambda_k (b_k - \sqrt{P}) + \mu \left( \frac{B_{\mathcal{D}_1}^2}{A} - \frac{B_{\mathcal{D}_2}^2}{A} + \Delta D \right)$$

of the optimization problem (15). From optimization theory, the second-order sufficient condition of optimality is known to be following.

*Proposition 1* (Second-order sufficient condition). If  $\nabla_{\mathbf{b}} \mathcal{L}(\mathbf{b}', \boldsymbol{\lambda}', \boldsymbol{\mu}') = \mathbf{0}$ , if  $\mathbf{b}'$  feasible, if strict complementarity holds, i.e.,  $\lambda'_k > 0, \forall k \in \bigcup_{m=1}^2 \mathcal{P}_m^C$  and if

$$\mathbf{s}^T \mathbf{H} \mathbf{s} > 0, \forall \mathbf{s} \in \mathcal{S} \triangleq \{\mathbf{s} \in \mathbb{R}^K : \mathbf{s} \neq \mathbf{0}, \mathbf{s}^T \nabla h(\mathbf{b}') = 0, \mathbf{s}^T \nabla g_k(\mathbf{b}') = 0, \forall k \in \bigcup_{m=1}^2 \mathcal{P}_m^C\}, \quad (22)$$

where  $\mathbf{H} = \nabla_{\mathbf{b}}^2 \mathcal{L}(\mathbf{b}', \boldsymbol{\lambda}', \boldsymbol{\mu}')$ , then it follows that  $\mathbf{b}'$  is a local minimizer.

Comparing  $\mathcal{S}$  in (22) with  $\mathcal{J}$  in (21), we see that  $\mathcal{S}$  is the kernel of  $\mathbf{J}^T$ , i.e.,  $\mathcal{S} = \ker(\mathbf{J}^T)$ . Note that  $\dim(\mathcal{S}) = K - \text{rank}(\mathbf{J})$  which simplifies to  $\dim(\mathcal{S}) = K - |\mathcal{P}_1^C| - |\mathcal{P}_2^C| - 1$ , if the LICQ is satisfied. Recall from linear algebra, that the *matrix inertia*  $\pi(\mathbf{H})$  of a symmetric  $K \times K$  real matrix is defined to be the triple  $(\rho, \eta, \theta)$ , where  $\rho, \eta$  and  $\theta$  are, respectively, the numbers of positive, negative and zero eigenvalues of the matrix  $\mathbf{H}$  with multiplicities counted [21]. *Han and Fujiwara* introduce the notion of *relative inertia*  $\pi(\mathbf{H}/\mathcal{S})$  for a symmetric  $K \times K$  real matrix [20]. They follow from Sylvester's law of inertia that

$$\pi(\mathbf{H}/\mathcal{S}) = \pi(\mathbf{S}^T \mathbf{H} \mathcal{S}), \quad (23)$$

where  $\mathcal{S}$  is a matrix whose columns form a basis of  $\mathcal{S}$ . One can infer that the second-order sufficient condition (22) is equivalent to the relative matrix inertia being  $\pi(\mathbf{H}/\mathcal{S}) = (\dim(\mathcal{S}), 0, 0)$ . However, examining the relative inertia may be tedious. A more practical approach is to check directly for the matrix inertia of the KKT-matrix

$$\mathbf{K} \triangleq \begin{bmatrix} \mathbf{H} & \mathbf{J} \\ \mathbf{J}^T & \mathbf{0} \end{bmatrix}. \quad (24)$$

To this end, *Han and Fujiwara* establish in [20, Theorem 3.4] for  $\theta(\mathbf{H}/\mathcal{S}) = 0^9$ , the direct relationship

$$\pi(\mathbf{K}) = \pi(\mathbf{H}/\mathcal{S}) + \left( \text{rank}(\mathbf{J}), \text{rank}(\mathbf{J}), |\mathcal{P}_1^C| + |\mathcal{P}_2^C| + 1 - \text{rank}(\mathbf{J}) \right).$$

For the KKT-point  $\mathbf{b}'$  which satisfies the LICQ such that  $\text{rank}(\mathbf{J}) = |\mathcal{P}_1^C| + |\mathcal{P}_2^C| + 1$  gives

$$\pi(\mathbf{K}) = \left( K, |\mathcal{P}_1^C| + |\mathcal{P}_2^C| + 1, 0 \right) \quad (25)$$

if  $\pi(\mathbf{H}/\mathcal{S}) = (K - |\mathcal{P}_1^C| - |\mathcal{P}_2^C| - 1, 0, 0)$ . Thus, in our simulation, to check for the second-order sufficient condition, we verify if (25) is satisfied.

<sup>9</sup>In Theorem 3.1, they show that  $\theta(\mathbf{K}) = \theta(\mathbf{H}/\mathcal{S}) + \dim(\ker(\mathbf{J}))$ . In other words, if  $\theta(\mathbf{K}) = 0 \implies \theta(\mathbf{H}/\mathcal{S}) = 0$ .

## V. SIMULATION RESULTS

In this section, we provide simulation results for validation of our proposed solution of optimization problem (11). Thus, we implicitly assume that the orthogonalization principle in computation described in III is deployed. Then, without loss of generality, we can focus on the real processing chain. We stick to the notation used in section IV. In the simulation, we model the absolute values of the channel coefficients  $h_k$  (which is actually  $|h_k|$ ) by i.i.d. Rayleigh fading, i.e.,  $h_k \sim \text{Rayl}(\sigma_R)$ , where  $\sigma_R$  is the scale parameter of the Rayleigh distribution. Then the mean and variance of  $h_k$ ,  $\forall k \in [1 : K]$ , are, respectively,  $\mu_h = \sigma_R \sqrt{\pi/2}$  and  $\sigma_h^2 = \frac{(4-\pi)}{2} \sigma_R^2$ . If not otherwise specified, we choose  $\sigma_h^2 = 1$ , while we set the noise variance to  $\sigma^2 = 1$ . For a *fixed* realization of  $(\mathcal{D}_1, \mathcal{D}_2)$ , where  $\mathcal{D}_m \subseteq [1 : K]$ ,  $\forall m \in [1 : 2]$ , with  $K = 30$ , we compute the normalized average MSE –  $\mathbb{E}_h[\text{MSE}] / \max(|\mathcal{D}_1|, |\mathcal{D}_2|)$  – for different SNR =  $P/\sigma^2$  in the range of –5 dB up to 50 dB in 5 dB increments. Note that for a fixed realization of  $(\mathcal{D}_1, \mathcal{D}_2)$ , we approximate  $\mathbb{E}_h[\text{MSE}]$  as an average MSE over the number of *feasible* realizations. Clearly, this number is always less or equal to the number of channel realizations, which we fix to 7500.

### A. Feasibility

In this subsection, we discuss how (a) the SNR, (b) the cardinality vector  $(|\mathcal{D}_1|, |\mathcal{D}_2|)$  and (c) the channel statistics of  $h_k$  affect the feasibility of the optimization problem (15). To this end, we count the number of all feasible and infeasible realizations as we either increase (a) the SNR from –5 dB to 5 dB in 5 dB (additive) increments, (b) the cardinality ratio  $|\mathcal{D}_2|/|\Delta\mathcal{D}|$  or (c) the channel statistics  $(\mu_h, \sigma_h^2)$  of  $h_k$ ,  $\forall k$ . We can see in Fig. 2 that an increase of any of those parameters has a positive impact on the feasibility of the optimization problem. This is in accordance with the discussion of subsection IV-B. Optimization problems that are parametrized by either a low SNR, large cardinality imbalances  $|\Delta\mathcal{D}|$  or Rayleigh distributions with a low mean and a low standard deviation are prone to suffer from infeasibility. However, the plots in 2a-2c show that sufficiently large/small values of these parameters, e.g., SNR  $\geq 5$  dB or  $|\Delta\mathcal{D}| \leq 20$ , make the optimization problem almost always feasible.

### B. Optimal Cardinality Set $(|\mathcal{P}_1^*|, |\mathcal{P}_2^*|)$

In this section, we discuss the influence of the SNR and  $(|\mathcal{D}_1|, |\mathcal{D}_2|)$  on the optimal cardinality vector  $(|\mathcal{P}_1^*|, |\mathcal{P}_2^*|)$ . To this end, we plot histograms of  $(|\mathcal{P}_1^*|, |\mathcal{P}_2^*|)$  for  $(|\mathcal{D}_1|, |\mathcal{D}_2|) =$

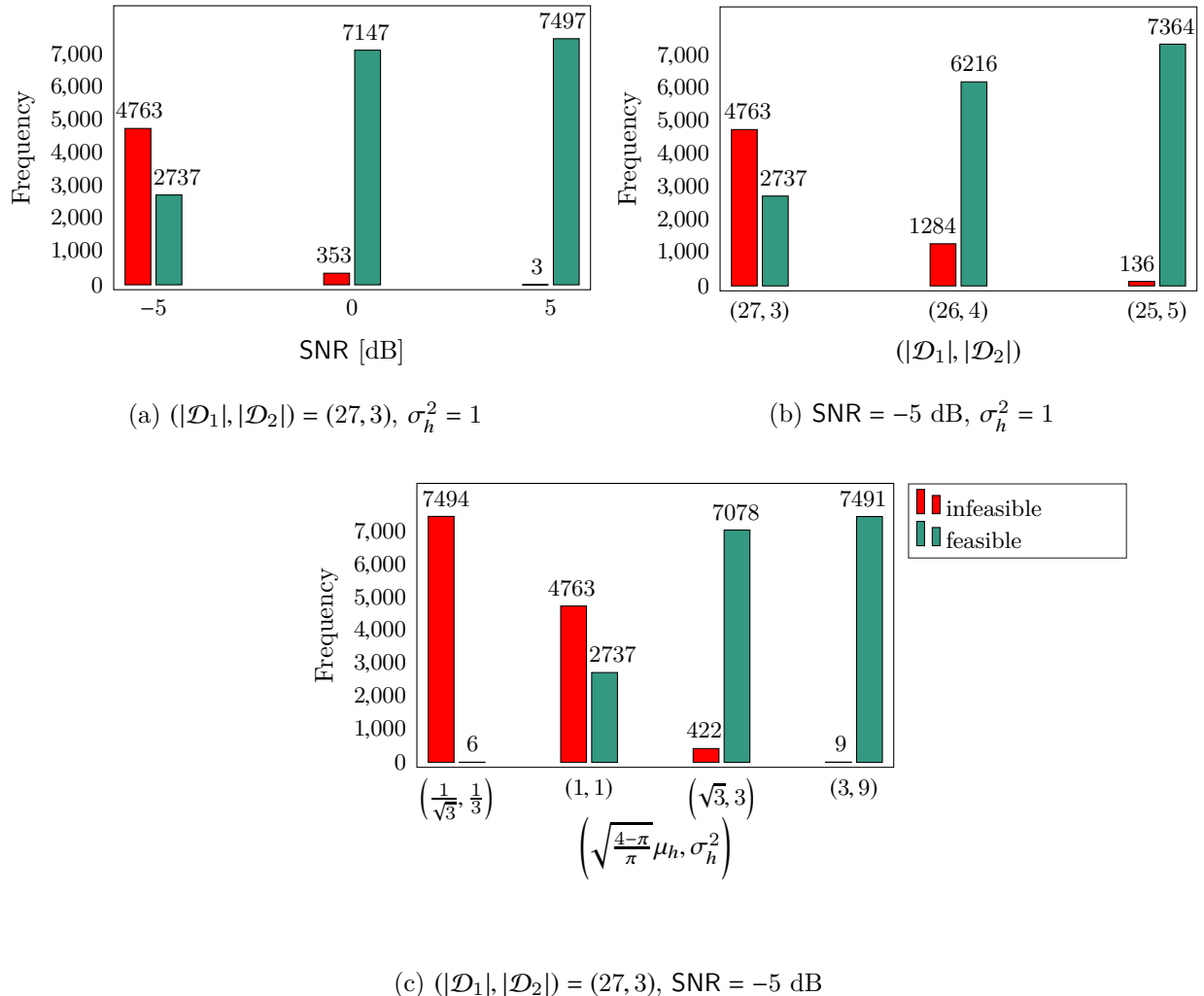


Fig. 2: Histogram of the number of infeasible (red) and feasible (green) realizations for varying (a) SNR, (b) cardinality vector  $(|\mathcal{D}_1|, |\mathcal{D}_2|)$  and (c) channel statistics  $(\mu_h, \sigma_h^2)$ . Recall that the noise variance is  $\sigma^2 = 1$  and that there are in total 7500 realizations.

(13, 17) (Fig. 3) and  $(|\mathcal{D}_1|, |\mathcal{D}_2|) = (22, 8)$  (Fig. 4) for  $\text{SNR} \in \{-5, 10, 30, 50\}$  dB. Qualitatively, at very high SNR, the distortion attributed to the interfering computation is dominant over the noise. For this case, letting all sensors transmit with full power is often detrimental for the accuracy in computation as it imposes significant interference. Rather, to limit the interference, we let only one single sensor – namely sensor  $\tilde{k}$  with its channel  $h_{\tilde{k}}$  matching the overall weakest channel  $h_{\min} \triangleq \min_{k \in [1:K]} h_k$  – transmit with full power; in other words, either  $(|\mathcal{P}_1^*|, |\mathcal{P}_2^*|) = (|\mathcal{D}_1|, |\mathcal{D}_2| - 1)$  or  $(|\mathcal{P}_1^*|, |\mathcal{P}_2^*|) = (|\mathcal{D}_1| - 1, |\mathcal{D}_2|)$ . The probability that  $\tilde{k} \in \mathcal{D}_m$  is  $\mathbb{P}(\tilde{k} \in \mathcal{D}_m) = |\mathcal{D}_m|/K$ . At SNR = 50 dB, we see in Fig. 3d (similarly for Fig.



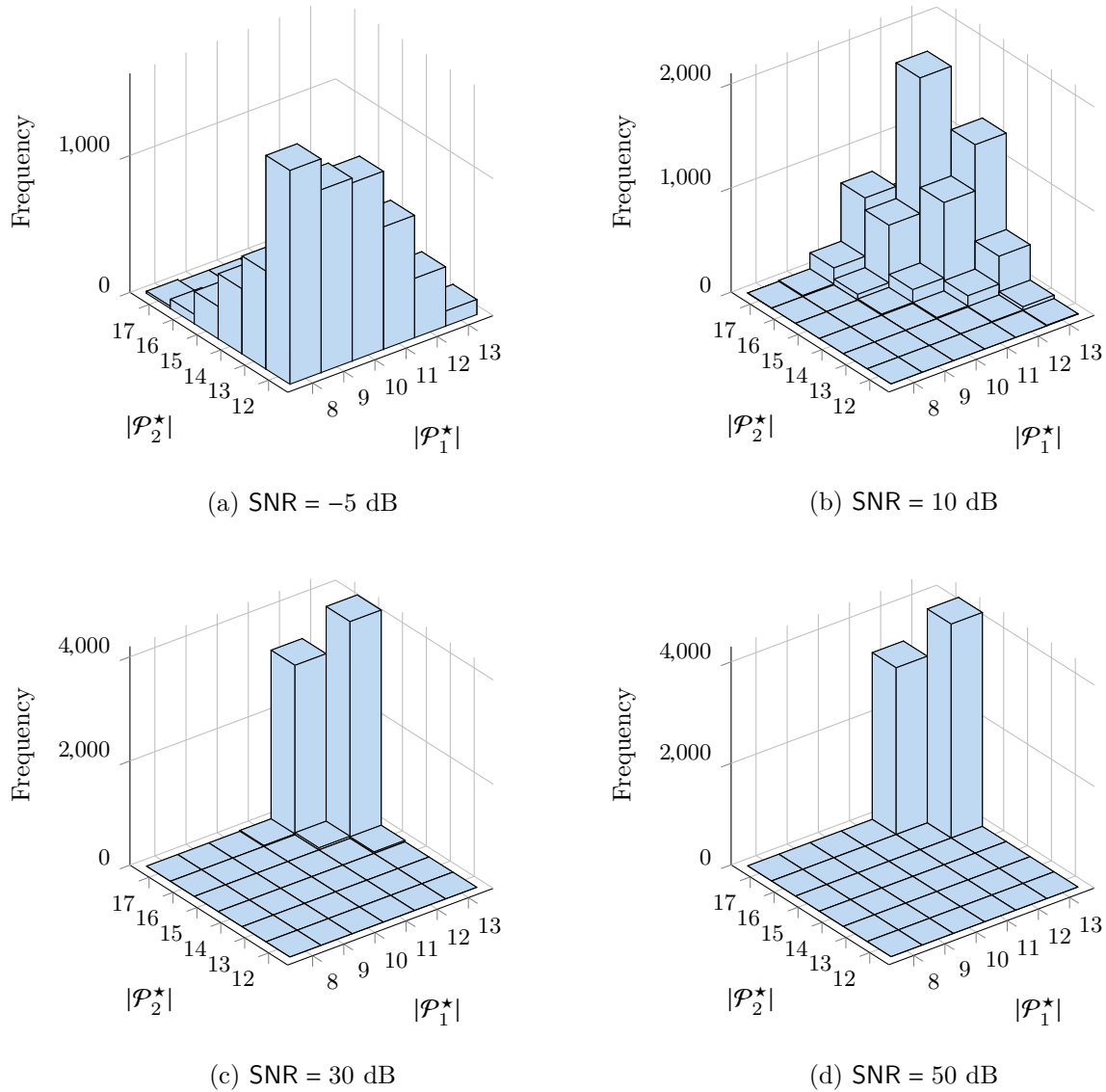


Fig. 3: Histogram of the optimal cardinality set  $(|\mathcal{P}_1^*|, |\mathcal{P}_2^*|)$  for  $(|\mathcal{D}_1|, |\mathcal{D}_2|) = (13, 17)$  and varying SNR  $\in \{-5, 10, 30, 50\}$  dB.

4d)) that  $(|\mathcal{P}_1^*|, |\mathcal{P}_2^*|) = (13, 16)$  or  $(|\mathcal{P}_1^*|, |\mathcal{P}_2^*|) = (12, 17)$  are the only optimal cardinality vectors which occur, respectively, with relative frequencies  $4215/7500$  ( $\approx \mathbb{P}(\tilde{k} \in \mathcal{D}_2) = 17/30$ ) and  $3285/7500$  ( $\approx \mathbb{P}(\tilde{k} \in \mathcal{D}_1) = 13/30$ ). As we decrease the SNR, irrespective of  $(|\mathcal{D}_1|, |\mathcal{D}_2|)$ , we observe that  $(|\mathcal{P}_1^*|, |\mathcal{P}_2^*|)$  becomes more dispersive. This observation implies that it is often better to let more sensors transmit with full power. Particularly, the lower the SNR, the more dispersion we observe in the histogram. For instance, while for SNR = 30 dB, the dispersion is almost non-existent, this effect is more prevalent for the histograms at SNR  $\in \{-5, 10\}$  dB.

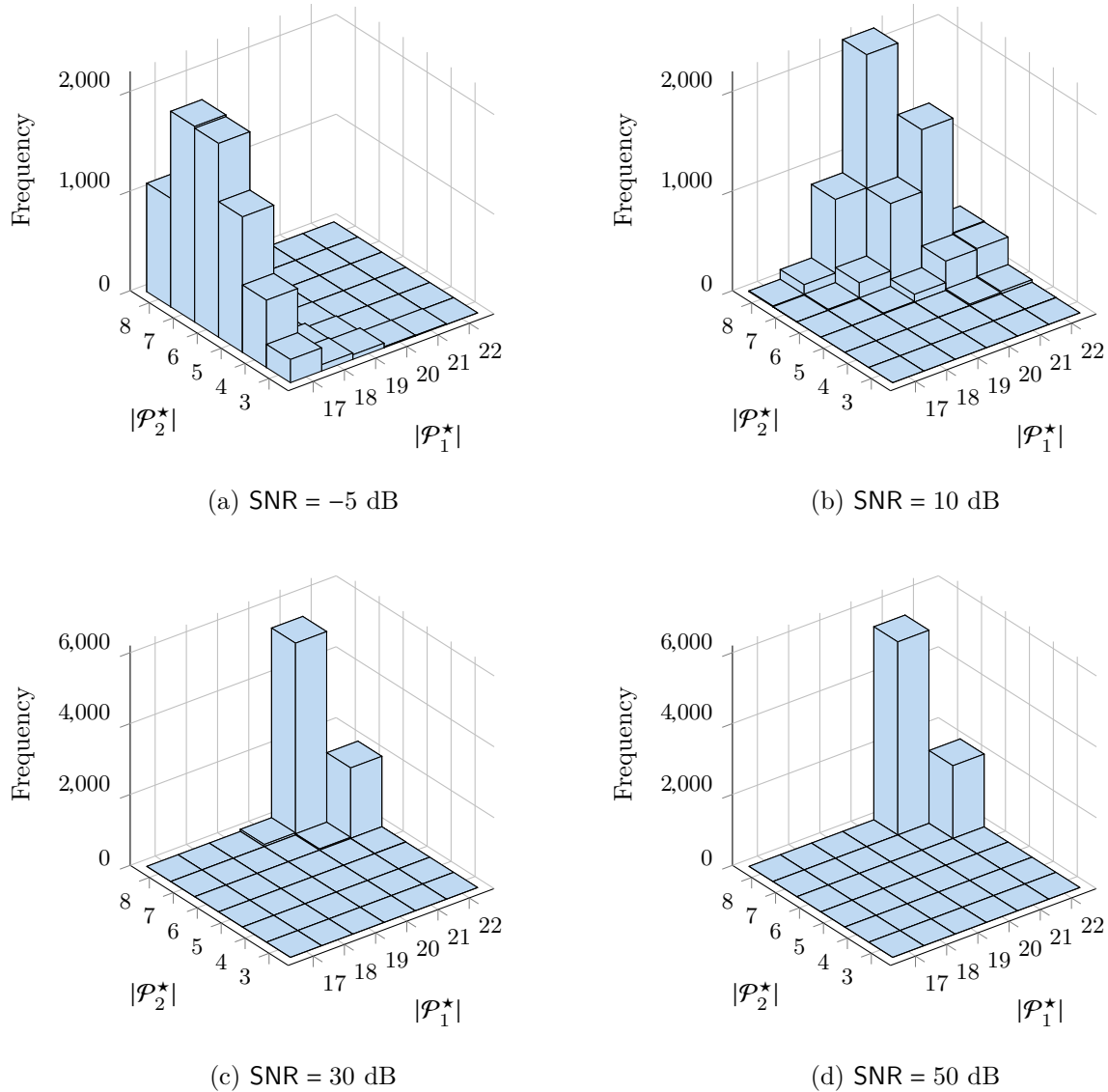


Fig. 4: Histogram of the optimal cardinality set  $(|\mathcal{P}_1^*|, |\mathcal{P}_2^*|)$  for  $(|\mathcal{D}_1|, |\mathcal{D}_2|) = (22, 8)$  and varying SNR  $\in \{-5, 10, 30, 50\}$  dB.

The histogram of SNR = 10 dB remains of similar shape as the ones for SNR  $\in \{30, 50\}$  dB. This is not the case for SNR = -5 dB where the effect of the noise is more dominant over the interference which allows more sensors to transmit with full power than at SNR  $\in \{10, 30, 50\}$  dB. This reflects in a drop of the cardinalities  $|\mathcal{P}_1^*|$  and  $|\mathcal{P}_2^*|$  (cf. Figs. 3a and 4a).

### C. Achievable Average MSE

Now, we elaborate on the behavior of the achievable, normalized MSE given by  $\mathbb{E}_h[\text{MSE}]/\max(|\mathcal{D}_1|, |\mathcal{D}_2|)$ .

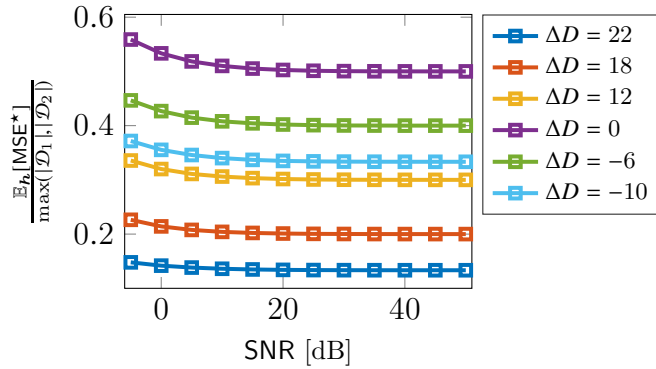


Fig. 5: The normalized, average MSE  $-\mathbb{E}_{\mathbf{h}}[\text{MSE}^*]/\max(|\mathcal{D}_1|, |\mathcal{D}_2|)$  versus SNR for different  $\Delta D$  realizations with  $K = 30$  sensors.

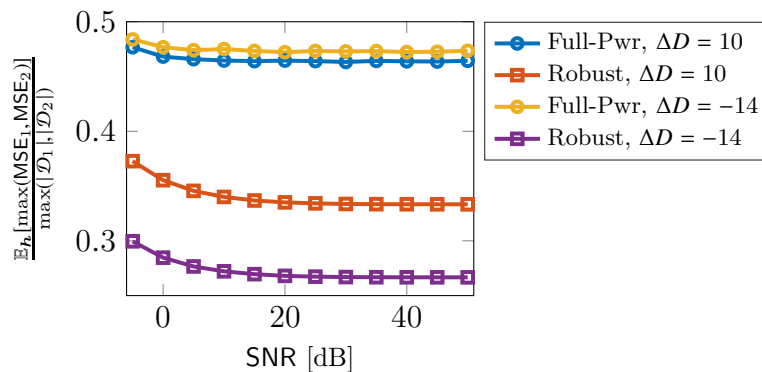


Fig. 6: Performance comparison between the robust MSE scheme of this paper with the full-power scheme ( $b_k = \sqrt{P}$ ,  $\forall k \in [1 : K]$ ).

Fig. 5 shows the average, normalized MSE over SNR. We see that irrespective of  $\Delta D$ , the average MSE is monotonously decreasing in SNR. However, for almost all channel realizations, the smaller  $|\Delta D|$ , the more interference is imposed on the calculation of  $s_m$  through the simultaneous computation of  $s_n$ ,  $m \neq n$ . In Fig. 5, this reflects on a decreasing behavior of the average MSE (independent of SNR) as we increase  $|\Delta D|$  from 0 to 22. In our simulations, we observe a symmetric behavior, i.e., for  $\Delta D$  and  $-\Delta D$ , the average MSEs are almost identical. As the SNR rises, we see in Fig. 5 that for all values of  $\Delta D$ , the normalized, average MSE converges. Interestingly, for  $\text{SNR} \rightarrow \infty$ , we infer from our simulation that the convergence limit becomes  $\mathbb{E}_{\mathbf{h}}[\text{MSE}^*] \rightarrow \frac{|\mathcal{D}_1||\mathcal{D}_2|}{K}$ . The normalized, average MSE for medium SNR ( $\text{SNR} \approx 10$  dB) is already close to this limit.

In Fig. 6, we compare the robust MSE scheme with a benchmark scheme, namely the full-power scheme, where  $\forall k \in [1 : K]$ ,  $b_k = \sqrt{P}$ , or in cardinality-sense  $(|\mathcal{P}_1|, |\mathcal{P}_2|) = (0, 0)$ . As already discussed, our scheme outperforms the full-power scheme. More detailed, the relative gain at  $\text{SNR} = -5$  dB ( $\text{SNR} = 50$  dB) for  $\Delta D = 10$  and  $\Delta D = -14$  are, respectively, 28% and 61% (39% and 77%). This increase in the relative gain from  $\text{SNR} = -5$  dB to  $\text{SNR} = 50$  dB is since the robust scheme much more resembles the full-power scheme at low  $\text{SNR}$  than at high  $\text{SNR}$ . This resemblance can be quantified by comparing the optimal cardinalities  $(|\mathcal{P}_1^*|, |\mathcal{P}_2^*|)$  at low and high  $\text{SNR}$  with  $(|\mathcal{P}_1|, |\mathcal{P}_2|) = (0, 0)$  of the benchmark scheme (cf. subsection V-B).

## VI. CONCLUDING REMARKS

In this work, we consider a multiple access channel (MAC) with  $K$  sensors as transmitters and a single receiver. For  $M$  mutually exclusive sensor index sets  $\mathcal{D}_m \subseteq [1 : K]$ ,  $\forall m \in [1 : M]$  of arbitrary cardinality, the MAC is used as a medium to compute the sums  $s_m = \sum_{k \in \mathcal{D}_m} x_k$ ,  $\forall m \in [1 : M]$ , of real-valued sensor observations  $x_k$  simultaneously. The goal is to minimize the worst-case, mean-squared error, i.e.,  $\max_{m \in [1 : M]} \text{MSE}_m$ , over all feasible Tx-Rx scaling policies  $(\mathbf{a}, \mathbf{b})$  subject to a Tx-power constraint. We show that an optimal design of the Tx-Rx scaling policy involves optimizing (a) their phases and (b) their absolute values to orthogonalize and minimize the computation over both real and imaginary part. The primary focus of this paper is on (b). We derive conditions (i) on the feasibility of the optimization problem and (ii) on the Tx-Rx scaling policy of a local minimum for  $M_R = 2$  computations over the real or the imaginary part. Extensive simulations show that the level of interference in terms of  $\Delta D = |\mathcal{D}_2| - |\mathcal{D}_1|$  plays an important role on the ergodic worst-case MSE. Interestingly, we observe that the ergodic worst-case MSE is not vanishing; rather, it converges to  $\frac{|\mathcal{D}_1| + |\mathcal{D}_2|}{K}$  as  $\text{SNR} \rightarrow \infty$ .

## APPENDIX A

### COMPARISON OF $\text{MSE}_m$ AND $\text{MSE}_{m,w}^\perp(C_w)$

Recall from section III that

$$\text{MSE}_m = \sum_{k \in \mathcal{D}_m} \left| |\bar{a}_m \tilde{b}_k| \cos(\phi_k - \alpha_m) - 1 \right|^2 + \sum_{\ell \in \mathcal{D}_m^C} \left| |\bar{a}_m \tilde{b}_\ell| \cos(\phi_\ell - \alpha_m) \right|^2 + \sigma^2 |\bar{a}_m|^2.$$

Naturally, the phase difference  $\phi_k - \alpha_m \in (-\pi/2, \pi/2)$  so that  $0 < \cos(\phi_k - \alpha_m) < 1$  and  $\text{MSE}_m < |\mathcal{D}_m|$ . Next, we define  $v_{km} \triangleq \left| |\bar{a}_m \tilde{b}_k| \cos(\phi_k - \alpha_m) - 1 \right|$  with its range being  $0 \leq v_{km} < 1$ . The *smallest*  $|\tilde{b}_k|^{10}$ ,  $k \in \mathcal{D}_m$ , that attains  $v_{km}$  is

$$|\tilde{b}_k| = \frac{1 - v_{km}}{|\bar{a}_m| \cos(\phi_k - \alpha_m)}.$$

Due to the power constraint  $|\tilde{b}_k| \leq h_k \sqrt{P}$ , or equivalently

$$v_{km} \geq 1 - |\bar{a}_m| h_k \cos(\phi_k - \alpha_m) \sqrt{P},$$

we can refine the range of  $v_{km}$  to be

$$\left[ 1 - |\bar{a}_m| h_k \cos(\phi_k - \alpha_m) \sqrt{P} \right]^+ \leq v_{km} \leq 1. \quad (26)$$

Now, we may rewrite  $\text{MSE}_m$  in terms of  $v_{km}$  as follows.

$$\widetilde{\text{MSE}}_m = \sum_{k \in \mathcal{D}_m} v_{km}^2 + \sum_{\substack{n=1 \\ n \neq m}}^M \left( \sum_{\ell \in \mathcal{D}_n} \frac{|\bar{a}_m|^2 (1 - v_{\ell n})^2 \cos^2(\phi_\ell - \alpha_m)}{|\bar{a}_n|^2 \cos^2(\phi_\ell - \alpha_n)} \right) + \sigma^2 |\bar{a}_m|^2. \quad (27)$$

We infer that the initial optimization problem (7) is equivalent to

$$\min_{\substack{\alpha, \phi, \\ \mathbf{a}', \mathbf{v}}} \max_{m \in [1:M]} \widetilde{\text{MSE}}_m \quad (28a)$$

$$\text{subject to} \quad (26), \quad \forall k \in \mathcal{D}_m, \forall m \in [1:M]. \quad (28b)$$

for  $\boldsymbol{\alpha} = [\alpha_1, \dots, \alpha_M]^T$ ,  $\boldsymbol{\phi} = [\phi_1, \dots, \phi_K]^T$ ,  $\mathbf{a}' = [|\bar{a}_1|, \dots, |\bar{a}_M|]^T$  and  $\mathbf{v} = (v_{km})_{k \in \mathcal{D}_m, m \in [1:M]}$ . Choosing  $\phi_\ell - \alpha_n = u\pi$ ,  $u \in \mathbb{Z}$ ,  $\forall \ell \in \mathcal{D}_n$ <sup>11</sup> has the following two positive effects. Namely, (i) we find a tight lower bound  $\widetilde{\text{MSE}}'_m$ ,  $\forall m \in [1:M]$  given by

$$\widetilde{\text{MSE}}'_m = \sum_{k \in \mathcal{D}_m} v_{km}^2 + \sum_{\substack{n=1 \\ n \neq m}}^M \left( \frac{|\bar{a}_m|^2 \cos^2(\alpha_n - \alpha_m)}{|\bar{a}_n|^2} \sum_{\ell \in \mathcal{D}_n} (1 - v_{\ell n})^2 \right) + \sigma^2 |\bar{a}_m|^2, \quad (29)$$

since  $\frac{\cos^2(\phi_\ell - \alpha_m)}{\cos^2(\phi_\ell - \alpha_n)} \geq \cos^2(\phi_\ell - \alpha_m)$  and (ii) the range of  $v_{\ell n}$  (cf. (26)) is maximized because  $1 - |\bar{a}_n| h_\ell \cos(\phi_\ell - \alpha_n) \sqrt{P} \geq 1 - |\bar{a}_n| h_\ell \sqrt{P}$  so that

$$\left[ 1 - |\bar{a}_n| h_\ell \sqrt{P} \right]^+ \leq v_{\ell n} \leq 1. \quad (30)$$

Note that this choice can, if anything, improve upon the optimal MSE. We observe that (29) depends on  $\cos^2(\Delta\alpha_{nm})$ , where  $\Delta\alpha_{nm} \triangleq \alpha_n - \alpha_m$  is a phase difference. Due to the symmetric

<sup>10</sup>Another – but larger in magnitude – solution is  $|\tilde{b}_k| = \frac{1+v_{km}}{|\bar{a}_m| \cos(\phi_k - \alpha_m)}$ .

<sup>11</sup>This suggests that for  $u = 0$  and distinct  $\ell_1, \ell_2 \in \mathcal{D}_n$ ,  $\alpha_n = \phi_{\mathcal{D}_n} = \phi_{\ell_1} = \phi_{\ell_2}$ .

behavior of  $\cos^2(\Delta\alpha_{nm})$ , we can assume without loss of generality  $\forall m, n \in [1 : M]$  that  $\Delta\alpha_{nm} \in [-\pi/2, \pi/2]$ . This allows us represent each phase difference by a convex combination

$$\Delta\alpha_{nm} = \begin{cases} \lambda_{nm} \cdot 0 + (1 - \lambda_{nm}) \cdot \frac{\pi}{2} = \frac{\pi(1-\lambda_{nm})}{2} & \text{if } \Delta\alpha_{nm} \geq 0 \\ \lambda_{nm} \cdot 0 - (1 - \lambda_{nm}) \cdot \frac{\pi}{2} = -\frac{\pi(1-\lambda_{nm})}{2} & \text{if } \Delta\alpha_{nm} \leq 0 \end{cases} \quad (31)$$

for  $\lambda_{nm} \in [0, 1]$ . Exploiting (31) and the *concavity* of  $\cos^2(x)$  in  $x \in [-\pi/2, \pi/2]$ , we conclude that

$$\cos^2(\Delta\alpha_{nm}) \geq \lambda_{nm} \cos^2(0) + (1 - \lambda_{nm}) \cos^2\left(\frac{\pi}{2}\right) = \lambda_{nm}. \quad (32)$$

To exploit (32), we need an understanding of the mapping from  $\Delta\alpha_{nm}$  to  $\lambda_{nm}$ , i.e.,  $\Delta\alpha_{nm} \rightarrow \lambda_{nm}$  for  $\Delta\alpha_{nm} \in [-\pi/2, \pi/2]$  and  $\lambda_{nm} \in [0, 1]$ . To this end, due to (31) we observe the following mapping on  $\lambda_{nm}$  for  $m, n, o \in [1 : M]$

$$\Delta\alpha_{mn} + \Delta\alpha_{nm} = 0 \implies \lambda_{mn} - \lambda_{nm} = 0, \quad (33)$$

$$\Delta\alpha_{mm} = 0 \implies \lambda_{mm} = 1, \quad (34)$$

$$\Delta\alpha_{nm} = \Delta\alpha_{no} + \Delta\alpha_{om} \implies \lambda_{nm} = \chi_{nm}(\lambda_{no}, \lambda_{om}, \text{sign}\{\Delta\alpha_{no} \cdot \Delta\alpha_{om}\}), \quad (35)$$

where for  $\lambda_{no}, \lambda_{om} \in [0, 1]$ ,  $z \in \{-1, 0, 1\}$

$$\chi_{nm}(\lambda_{no}, \lambda_{om}, z) \triangleq \begin{cases} \chi_{nm}^{(z \geq 0)}(\lambda_{no}, \lambda_{om}) & \text{for } z \in \{0, 1\} \\ \chi_{nm}^{(z \leq 0)}(\lambda_{no}, \lambda_{om}) & \text{for } z \in \{-1, 0\} \end{cases} \quad (36)$$

with

$$\chi_{nm}^{(z \geq 0)}(\lambda_{no}, \lambda_{om}) \triangleq \begin{cases} 1 - \lambda_{no} - \lambda_{om} & \text{if } 0 \leq \lambda_{no} + \lambda_{om} \leq 1 \\ -1 + \lambda_{no} + \lambda_{om} & \text{if } 1 \leq \lambda_{no} + \lambda_{om} \leq 2 \end{cases},$$

$$\chi_{nm}^{(z \leq 0)}(\lambda_{no}, \lambda_{om}) \triangleq \begin{cases} 1 + \lambda_{no} - \lambda_{om} & \text{if } -1 \leq \lambda_{no} - \lambda_{om} \leq 0 \\ 1 - \lambda_{no} + \lambda_{om} & \text{if } 0 \leq \lambda_{no} - \lambda_{om} \leq 1 \end{cases}.$$

Wherever unnecessary, we omit the variable  $z$  of the function  $\chi_{nm}$ . Note that this function has the following properties:

- (a) range:  $0 \leq \chi_{nm} \leq 1$ ,
- (b) symmetry:  $\chi_{nm}(\lambda_{no}, \lambda_{om}, z) = \chi_{nm}(\lambda_{om}, \lambda_{no}, z)$ ,
- (c) optimum:

$$- \operatorname{argmin} \chi_{nm}^{(z \geq 0)}(\lambda_{no}, \lambda_{om}) = \{(\lambda_{no}, \lambda_{om}) \in [0, 1]^2 : \lambda_{no} + \lambda_{om} = 1\},$$

- $\operatorname{argmin} \chi_{nm}^{(z \leq 0)}(\lambda_{no}, \lambda_{om}) = \{(0, 1), (1, 0)\}$ ,
- $\operatorname{argmax} \chi_{nm}^{(z \geq 0)}(\lambda_{no}, \lambda_{om}) = \{(0, 0), (1, 1)\}$ ,
- $\operatorname{argmax} \chi_{nm}^{(z \leq 0)}(\lambda_{no}, \lambda_{om}) = \{(\lambda_{no}, \lambda_{om}) \in [0, 1]^2 : \lambda_{no} - \lambda_{om} = 0\}$ ,

(d) extreme points:

- $\chi_{nm}(\lambda_{no}, 0) = 1 - \lambda_{no}$ ,
- $\chi_{nm}(\lambda_{no}, 1) = \lambda_{no}$ ,
- $\chi_{nm}(0, 0) = \chi_{nm}(1, 1) = 1$ ,
- $\chi_{nm}(0, 1) = \chi_{nm}(1, 0) = 0$ .

Ultimately, using Eqs. (32), (33), (35) and (36), we can lower bound  $\widetilde{\text{MSE}}'_m$ ,  $\forall m \in [1 : M]$  and some  $o \in [1 : M] \setminus \{m\}$  by

$$\widetilde{\text{MSE}}''_m = \sum_{k \in \mathcal{D}_m} v_{km}^2 + \sum_{\substack{n=1 \\ n \neq m}}^M \left( \frac{|\bar{a}_m|^2}{|\bar{a}_n|^2} \chi_{nm}(\lambda_{on}, \lambda_{om}) \sum_{\ell \in \mathcal{D}_n} (1 - v_{\ell n})^2 \right) + \sigma^2 |\bar{a}_m|^2. \quad (37)$$

Due to the optimum property of  $\chi_{nm}$ , it is always best to choose  $(\lambda_{on}, \lambda_{om}) \in \{(0, 1), (1, 0)\}$ . Recall that  $\lambda_{on} = 0$  ( $\lambda_{on} = 1$ ) represents a phase difference of  $\Delta\alpha_{on} = \pi/2$  ( $\Delta\alpha_{on} = 0$ ). Ultimately, this leads to the orthogonalization strategy and the exhaustive search in (13) of the optimal computation index sets. Thus, in the optimum  $\text{MSE}_m$  and  $\text{MSE}_{m,w}^\perp(C_w)$  match.

## APPENDIX B

### LOWER BOUND ON $\text{MSE}_{m,C_R}^\perp$

Note that  $\text{MSE}_j \geq |\mathcal{D}_j| - B_{\mathcal{D}_j}^2/A$ . Thus for  $c_m \in \mathbb{R}_+$ ,  $|\mathcal{D}_1| - B_{\mathcal{D}_1}^2/A$  and  $|\mathcal{D}_2| - B_{\mathcal{D}_2}^2/A$  function as lower bounds on the worst-case MSE. Above observation implies that ideally, we would like to ensure that the lower bounds on the MSEs are tight, i.e.,

$$\text{MSE}_j = \text{MSE}_k = |\mathcal{D}_k| - B_{\mathcal{D}_k}^2/A = |\mathcal{D}_j| - B_{\mathcal{D}_j}^2/A. \quad (38)$$

## APPENDIX C

### KKT-CONDITIONS

The Lagrangian for the optimization problem of subsection IV-A with Lagrange multipliers  $\boldsymbol{\lambda} = (\lambda_1, \dots, \lambda_K)^T$  and  $\boldsymbol{\mu}$  is

$$\mathcal{L}(\mathbf{b}, \boldsymbol{\lambda}, \boldsymbol{\mu}) = \underbrace{-\frac{B_{\mathcal{D}_1}^2}{A}}_{\triangleq f_0(\mathbf{b})} + \sum_{k=1}^K \lambda_k \underbrace{\left( b_k - \sqrt{P} \right)}_{\triangleq g_k(\mathbf{b})} + \boldsymbol{\mu} \underbrace{\left( \frac{B_{\mathcal{D}_1}^2}{A} - \frac{B_{\mathcal{D}_2}^2}{A} + \Delta D \right)}_{\triangleq h(\mathbf{b})}.$$

To derive the KKT-conditions, we first determine the partial derivative

$$\frac{\partial \mathcal{L}}{\partial b_k} = \begin{cases} -\frac{2B_{\mathcal{D}_1} h_k}{A^2} (A - h_k b_k B_{\mathcal{D}_1}) (1 - \mu) + \frac{2B_{\mathcal{D}_2}^2}{A^2} h_k^2 b_k \mu + \lambda_k & \text{if } k \in \mathcal{D}_1 \\ \frac{2B_{\mathcal{D}_1}^2}{A^2} h_k^2 b_k (1 - \mu) - \frac{2B_{\mathcal{D}_2} h_k \mu}{A^2} (A - h_k b_k B_{\mathcal{D}_2}) + \lambda_k & \text{if } k \in \mathcal{D}_2 \end{cases}. \quad (39)$$

Then, the KKT-conditions are as follows.

$$\nabla_{\mathbf{b}} \mathcal{L} = \mathbf{0} \quad (\text{stationarity}) \quad (40)$$

$$g_k(\mathbf{b}) \leq 0, \forall k \in [1 : K] \quad (\text{inequality feasibility constraint}) \quad (41)$$

$$h(\mathbf{b}) = 0 \quad (\text{equality feasibility constraint}) \quad (42)$$

$$\boldsymbol{\lambda} \geq \mathbf{0} \quad (\text{dual feasibility}) \quad (43)$$

$$\lambda_k g_k(\mathbf{b}) = 0, \forall k \in [1 : K] \quad (\text{complementary slackness}) \quad (44)$$

#### APPENDIX D

##### SOLUTION TO KKT-CONDITIONS (40)–(44)

Note that the complementary slackness condition (44) suggests that a KKT-point  $\mathbf{b}'$  has entries  $b_k < \sqrt{P}$  and  $b_k = \sqrt{P}$ . The subsets  $\mathcal{P}_m$  and  $\mathcal{P}_m^C$  of  $\mathcal{D}_m$ ,  $\forall m \in [1 : 2]$ , indicate which of the sensors in  $\mathcal{D}_m$  transmit with full power and less-than full power. Further, for the latter type of sensors, their respective Lagrange multipliers are  $\lambda_k = 0$ ,  $\forall k \in \mathcal{P}_m$ . If  $\mathcal{P}_m \neq \emptyset$ , then we define for  $j \in \mathcal{P}_m$

$$E_{\mathcal{P}_m} = h_j b_j, \quad (45)$$

such that

$$B_{\mathcal{D}_m} = |\mathcal{P}_m| E_{\mathcal{P}_m} + \sqrt{P} h'_m, \quad (46)$$

$$A = \sigma^2 + \sum_{m=1}^2 \left( |\mathcal{P}_m| E_{\mathcal{P}_m}^2 + P h_{sm} \right), \quad (47)$$

where  $h'_m = \sum_{k \in \mathcal{P}_m^C} h_k$  and  $h_{sm} = \sum_{k \in \mathcal{P}_m^C} h_k^2$ . We emphasize that in the case of  $\mathcal{P}_m = \emptyset$  ( $\mathcal{P}_m^C = \emptyset$ ),  $E_{\mathcal{P}_m} = 0$  ( $h'_m = h_{sm} = 0, \forall m \in [1 : 2]$ ). The equality feasibility constraint (42) in



terms of  $(E_{\mathcal{P}_1}, E_{\mathcal{P}_2})$  becomes the following.

$$\frac{B_{\mathcal{D}_2}^2}{A} - \frac{B_{\mathcal{D}_1}^2}{A} = \Delta D \stackrel{(45),(46),(47)}{\iff} \begin{cases} |\mathcal{P}_2|E_{\mathcal{P}_2} - |\mathcal{P}_1|E_{\mathcal{P}_1} + \sqrt{P}(h'_2 - h'_1) = 0 & \text{if } \Delta D = 0 \\ \left( |\mathcal{P}_2|E_{\mathcal{P}_2} + \sqrt{P}h'_2 \right)^2 - \left( |\mathcal{P}_1|E_{\mathcal{P}_1} + \sqrt{P}h'_1 \right)^2 \\ - \Delta D \left( \sigma^2 + \sum_{m=1}^2 \left( |\mathcal{P}_m|E_{\mathcal{P}_m}^2 + Ph_{sm} \right) \right) = 0 & \text{if } \Delta D \neq 0 \end{cases}. \quad (48)$$

The condition (40) gives us the following expressions on  $\mu$ .

$$\mu = \begin{cases} \frac{B_{\mathcal{D}_1}(A - h_k b_k B_{\mathcal{D}_1})}{A(h_k b_k \Delta D + B_{\mathcal{D}_1})} - \frac{\lambda_k A}{2h_k(h_k b_k \Delta D + B_{\mathcal{D}_1})} & \text{if } k \in \mathcal{D}_1 \\ \frac{h_k b_k (B_{\mathcal{D}_2}^2 - A \Delta D)}{A(B_{\mathcal{D}_2} - h_k b_k \Delta D)} + \frac{\lambda_k A}{2h_k(B_{\mathcal{D}_2} - h_k b_k \Delta D)} & \text{if } k \in \mathcal{D}_2 \end{cases} \quad (49)$$

We need to ensure that the two expressions on  $\mu$  for  $k \in \mathcal{D}_1$  and  $k \in \mathcal{D}_2$  in (49) are of the same value. With Eqs. (45), (46), (47), the definitions on  $\mathcal{P}_m$  and  $\mathcal{P}_m^C$ , this is the case for  $(E_{\mathcal{P}_1}, E_{\mathcal{P}_2})$  and  $\lambda_k, \forall k \in \mathcal{P}_m^C, m \in [1 : 2]$ , if the following set of equations are satisfied.

$$\frac{2B_{\mathcal{D}_m}B_{\mathcal{D}_n}^2}{A^2(B_{\mathcal{D}_m} + (-1)^{m+1}E_{\mathcal{P}_m}\Delta D)} \left( h_k \sqrt{P} - E_{\mathcal{P}_m} \right) = -\frac{\lambda_k}{h_k} \text{ for } j \in \mathcal{P}_m, k \in \mathcal{P}_m^C, m \neq n, \quad (50)$$

$$\begin{aligned} \frac{2B_{\mathcal{D}_m}B_{\mathcal{D}_n}^2}{A^2} \sqrt{P} (h_k - h_j) &= B_{\mathcal{D}_m} \left( \frac{\lambda_j}{h_j} - \frac{\lambda_k}{h_k} \right) \\ + (-1)^{m+1} \Delta D \sqrt{P} \left( \frac{\lambda_j}{h_j} h_k - \frac{\lambda_k}{h_k} h_j \right) &\text{ for } j, k \in \mathcal{P}_m^C, m \neq n \end{aligned} \quad (51)$$

$$E_{\mathcal{P}_1} B_{\mathcal{D}_1} + E_{\mathcal{P}_2} B_{\mathcal{D}_2} = A \text{ for } j \in \mathcal{P}_1, k \in \mathcal{P}_2, \quad (52)$$

$$\frac{2B_{\mathcal{D}_1}B_{\mathcal{D}_2}}{A^2} \left( \frac{A - h_j \sqrt{P} B_{\mathcal{D}_m} - E_{\mathcal{P}_n} B_{\mathcal{D}_n}}{B_{\mathcal{D}_n} + (-1)^i E_{\mathcal{P}_n} \Delta D} \right) = \frac{\lambda_j}{h_j} \text{ for } j \in \mathcal{P}_m^C, k \in \mathcal{P}_n, m \neq n, \quad (53)$$

$$\begin{aligned} \frac{2B_{\mathcal{D}_1}B_{\mathcal{D}_2}}{A^2} \left( A - \sqrt{P} (h_j B_{\mathcal{D}_1} + h_k B_{\mathcal{D}_2}) \right) &= \frac{\lambda_j}{h_j} B_{\mathcal{D}_2} + \frac{\lambda_k}{h_k} B_{\mathcal{D}_1} \\ - \Delta D \sqrt{P} \left( \frac{\lambda_j}{h_j} h_k - \frac{\lambda_k}{h_k} h_j \right) &\text{ for } j \in \mathcal{P}_1^C, k \in \mathcal{P}_2^C. \end{aligned} \quad (54)$$

Now, we iterate through all possible cardinality vectors  $(|\mathcal{P}_1|, |\mathcal{P}_2|)$ , where every cardinality  $|\mathcal{P}_m|, |\mathcal{P}_m^C| \geq 0$  satisfies

$$|\mathcal{P}_m| + |\mathcal{P}_m^C| = |\mathcal{D}_m|.$$

For each of those choices, we design  $\mathcal{P}_m$  and determine  $(E_{\mathcal{P}_1}, E_{\mathcal{P}_2})$  as well as the Lagrange multipliers  $\lambda_k, k \in \mathcal{P}_m^C, m \in [1 : 2]$ , from Eqs. (48), (50), (51), (52), (53) and (54). We start

with the two extreme cases, where *a*) no sensor transmits with full power, i.e.,  $(|\mathcal{P}_1|, |\mathcal{P}_2|) = (|\mathcal{D}_1|, |\mathcal{D}_2|)$  and *b*) all sensors transmit with full power, i.e.,  $(|\mathcal{P}_1|, |\mathcal{P}_2|) = (0, 0)$ . Then, we study intermediate cases of *a*) and *b*). Namely, we consider *c*) cardinalities  $(|\mathcal{P}_1|, |\mathcal{P}_2|) \geq (1, 1)$  (excluding the extreme case *a*)) and finally *d*)  $|\mathcal{P}_m| \geq 1$  and  $|\mathcal{P}_n| = 0$  for  $m \neq n$ .

*a) a*)  $(|\mathcal{P}_1|, |\mathcal{P}_2|) = (|\mathcal{D}_1|, |\mathcal{D}_2|)$ :: Since  $\sigma^2 > 0$ , (52) is never satisfied for this case. Hence, irrespective of  $\Delta D$ , this case does not produce a KKT-point.

*b) b*)  $(|\mathcal{P}_1|, |\mathcal{P}_2|) = (0, 0)$ :: We can check for  $(E_{\mathcal{P}_1}, E_{\mathcal{P}_2}) = (0, 0)$  in (48) that only degenerate channel conditions satisfy the equality constraint. For channel coefficients drawn from a continuous distributions, these degenerate conditions occur with zero probability.

*c) c*)  $(|\mathcal{P}_1|, |\mathcal{P}_2|) \geq (1, 1)$ :: For this case, we determine  $(E_{\mathcal{P}_1}, E_{\mathcal{P}_2})$  by solving the system of equations (48) and (52) which is either linear if  $\Delta D = 0$  or quadratic otherwise ( $\Delta D \neq 0$ ). For the special case  $\Delta D = 0$ , we find a rather short, real-valued expression on  $E_{\mathcal{P}_m}$  for  $m \neq n$  and  $\Delta h = h'_2 - h'_1$ .

$$E_{\mathcal{P}_m}^{(\Delta D=0)} = \frac{|\mathcal{P}_n| (\sigma^2 + P (h_{s1} + h_{s2})) + (-1)^n P (\Delta h) h'_n}{\sqrt{P} (|\mathcal{P}_1| h'_2 + |\mathcal{P}_2| h'_1)} \quad (55)$$

However, for  $\Delta D \neq 0$ , the solution is lengthy and omitted here for ease of presentation. We remind the reader that only real and non-negative solutions are allowed. Assuming the existence of a real solution vector  $(E_{\mathcal{P}_1}, E_{\mathcal{P}_2})$ , which only depends on  $\mathbf{h}$ ,  $\sigma^2$ ,  $P$ ,  $\Delta D$  and  $|\mathcal{P}_m|$ , we can infer from (45), (50), (51), (53), (54) that

$$b_j = \frac{E_{\mathcal{P}_m}}{h_j}, \quad (56)$$

$$\lambda_k = \frac{2B_{\mathcal{D}_m} B_{\mathcal{D}_n}^2}{A^2 (B_{\mathcal{D}_m} + (-1)^{m+1} E_{\mathcal{P}_m} \Delta D)} h_k (E_{\mathcal{P}_m} - h_k \sqrt{P}), \quad (57)$$

for  $j \in \mathcal{P}_m$  and  $k \in \mathcal{P}_m^C$ ,  $\forall m \in [1 : 2]$ .

*d) d*)  $|\mathcal{P}_m| \geq 1, |\mathcal{P}_n| = 0$ :: For this case, we solve for  $E_{\mathcal{P}_m}$  in (48) when  $E_{\mathcal{P}_n} = 0$ . Again, in the interest of simplicity, we only state the explicit expression for  $\Delta D = 0$  (and omit the one for  $\Delta D \neq 0$ ).

$$E_{\mathcal{P}_m}^{(\Delta D=0)} = \frac{(-1)^n \sqrt{P} (\Delta h)}{|\mathcal{P}_m|} \quad (58)$$

A given  $E_{\mathcal{P}_m}$  allows us to compute the primal and dual variables for  $j \in \mathcal{P}_m$ ,  $k \in \mathcal{P}_m^C$  and  $\ell \in \mathcal{P}_n^C$  according to

$$\begin{aligned} b_j &= \frac{E_{\mathcal{P}_m}}{h_j}, \\ \lambda_k &= \frac{2B_{\mathcal{D}_m}B_{\mathcal{D}_n}^2}{A^2(B_{\mathcal{D}_m} + (-1)^{m+1}E_{\mathcal{P}_m}\Delta D)} h_k (E_{\mathcal{P}_m} - h_k\sqrt{P}), \\ \lambda_\ell &= \frac{2B_{\mathcal{D}_1}B_{\mathcal{D}_2}}{A^2} \left( \frac{A - E_{\mathcal{P}_m}B_{\mathcal{D}_m} - h_\ell\sqrt{P}B_{\mathcal{D}_n}}{B_{\mathcal{D}_m} + (-1)^{m+1}E_{\mathcal{P}_m}\Delta D} \right). \end{aligned} \quad (59)$$

So far, we have computed  $E_{\mathcal{P}_m}$  and  $\lambda_k$  for cases  $c)$  and  $d)$ . Wherever necessary, to distinguish their values, we use the subscripts  $c)$  and  $d)$  for  $E_{\mathcal{P}_m}$ . For  $j \in \mathcal{P}_m$ , we know from (41) that  $b_j \in [0, \sqrt{P})$ . This suggests that for  $j \in \mathcal{P}_m$ , and cases  $c)$  and  $d)$  that

$$0 \leq E_{\mathcal{P}_m} < h_j\sqrt{P}. \quad (60)$$

Simultaneously, the dual feasibility constraint  $\boldsymbol{\lambda} \geq \mathbf{0}$  confines the range of  $E_{\mathcal{P}_m}$  further. The Lagrange multipliers of cases  $c)$  and  $d)$  (cf. (57) and (59)) are fractions  $\text{num}/\text{den}$  with the same common denominator  $\text{den}$  but potentially a different numerator  $\text{num}$ . Clearly,  $\lambda_k > 0$  is equivalent to either  $\{\text{num} > 0, \text{den} > 0\}$  or  $\{\text{num} < 0, \text{den} < 0\}$ . Without going into details, this gives us ultimately the following conditions on  $E_{\mathcal{P}_m}$  for  $k \in \mathcal{P}_m^C$  and

- case  $c)$ ,  $\forall m, n \in [1 : 2], m \neq n$ :

$$\begin{cases} h_k\sqrt{P} < E_{\mathcal{P}_{m,c}} & \text{if } |\mathcal{D}_n| \geq |\mathcal{P}_m^C| \\ h_k\sqrt{P} < E_{\mathcal{P}_{m,c}} < \frac{\sqrt{P}h'_m}{|\mathcal{P}_m^C| - |\mathcal{D}_n|} & \text{if } |\mathcal{D}_n| < |\mathcal{P}_m^C| \end{cases}, \quad (61)$$

- case  $d)$ ,  $\ell \in \mathcal{P}_n^C, m \neq n$ :

$$\begin{cases} h_k\sqrt{P} < E_{\mathcal{P}_{m,d}} < \frac{\sigma^2 + P(h_{s1} + h_{s2} - h_\ell h'_n)}{\sqrt{P}h'_m} & \text{if } |\mathcal{D}_n| \geq |\mathcal{P}_m^C| \\ h_k\sqrt{P} < E_{\mathcal{P}_{m,d}} < \min\left(\frac{\sigma^2 + P(h_{s1} + h_{s2} - h_\ell h'_n)}{\sqrt{P}h'_m}, \frac{\sqrt{P}h'_m}{|\mathcal{P}_m^C| - |\mathcal{D}_n|}\right) & \text{if } |\mathcal{D}_n| < |\mathcal{P}_m^C| \end{cases}. \quad (62)$$

We would like to highlight to the reader that typically *strict complementarity*, i.e.,  $\lambda_k > 0$ ,  $\forall k \in \mathcal{P}_m^C, m \in [1 : 2]$ , holds, since the sets in (61) and (62) constraining  $E_{\mathcal{P}_m}$  are usually open. The case where  $E_{\mathcal{P}_m}$  matches with the right-hand or left-hand side of the inequalities (which causes  $\lambda_k = 0$ ) happens only for degenerate channel conditions which have zero probability. This observation is needed when we consider the second-order sufficient condition.

Combining (60), (61) and (62) gives us the final conditions on  $E_{\mathcal{P}_m}$  such that the vector  $\mathbf{b}' = (b'_1, \dots, b'_K)^T$  with its  $k$ -th element corresponding to

$$b'_k = \begin{cases} \sqrt{P} & \text{if } k \in \bigcup_{m=1}^2 \mathcal{P}_m^C, \\ \frac{E_{\mathcal{P}_m}}{h_k} & \text{if } k \in \bigcup_{m=1}^2 \mathcal{P}_m, \end{cases} \quad (63)$$

becomes a feasible KKT-point. Further, the combination of these conditions suggests that the largest  $|\mathcal{P}_m| \leq |\mathcal{D}_m|$  channel coefficients of  $\mathbf{h}_{\mathcal{D}_m} \triangleq (h_k)_{k \in \mathcal{D}_m}$  generate the vector  $\mathbf{h}_{\mathcal{P}_m} \triangleq (h_k)_{k \in \mathcal{P}_m}$ , i.e.,

$$\mathbf{h}_{\mathcal{P}_m} = \left( \mathbf{h}_{\mathcal{D}_{m[k]}} \right)_{k=1}^{|\mathcal{P}_m|},$$

where  $\mathbf{h}_{\mathcal{D}_{m[k]}}$  is the  $k$ -th largest component of  $\mathbf{h}_{\mathcal{D}_m}$  and  $\mathcal{P}_m$  the respective index set of  $\mathbf{h}_{\mathcal{P}_m}$  from  $[1 : K]$ . The remaining  $|\mathcal{P}_m^C|$  channel coefficients of  $\mathbf{h}_{\mathcal{D}_m}$  form  $\mathbf{h}_{\mathcal{P}_m^C}$ . Defining  $\bar{\mathbf{v}}_m = \mathbf{h}_{\mathcal{D}_{m[|\mathcal{P}_m|]}}$ ,  $\underline{\mathbf{v}}_m = \mathbf{h}_{\mathcal{D}_{m[|\mathcal{P}_m|+1]}}$  and  $\bar{\mathbf{w}}_n = \mathbf{h}_{\mathcal{D}_{n[1]}}$  allows us to compactly write the condition on  $E_{\mathcal{P}_m}$  such that primal and dual feasibility hold. This gives us for

- case c),  $\forall m, n \in [1 : 2], m \neq n$ :

$$\begin{cases} \underline{\mathbf{v}}_m \sqrt{P} < E_{\mathcal{P}_{m,c}} < \bar{\mathbf{v}}_m \sqrt{P} & \text{if } |\mathcal{D}_n| \geq |\mathcal{P}_m^C|, \\ \underline{\mathbf{v}}_m \sqrt{P} < E_{\mathcal{P}_{m,c}} < \min \left( \bar{\mathbf{v}}_m \sqrt{P}, \frac{\sqrt{P} h'_m}{|\mathcal{P}_m^C| - |\mathcal{D}_n|} \right) & \text{if } |\mathcal{D}_n| < |\mathcal{P}_m^C|, \end{cases} \quad (64)$$

- case d),  $m \neq n$ :

$$\begin{cases} \underline{\mathbf{v}}_m \sqrt{P} < E_{\mathcal{P}_{m,d}} < \min \left( \bar{\mathbf{v}}_m \sqrt{P}, \frac{\sigma^2 + P(h_{s1} + h_{s2} - \bar{\mathbf{w}}_n h'_n)}{\sqrt{P} h'_m} \right) & \text{if } |\mathcal{D}_n| \geq |\mathcal{P}_m^C|, \\ \underline{\mathbf{v}}_m \sqrt{P} < E_{\mathcal{P}_{m,d}} < \min \left( \bar{\mathbf{v}}_m \sqrt{P}, \frac{\sigma^2 + P(h_{s1} + h_{s2} - \bar{\mathbf{w}}_n h'_n)}{\sqrt{P} h'_m}, \frac{\sqrt{P} h'_m}{|\mathcal{P}_m^C| - |\mathcal{D}_n|} \right) & \text{if } |\mathcal{D}_n| < |\mathcal{P}_m^C|. \end{cases} \quad (65)$$

## APPENDIX E

### VERIFICATION OF THE LINEAR INDEPENDENCE CONSTRAINT QUALIFICATION (LICQ)

Recall that the LICQ holds at  $\mathbf{b}'$ , iff  $\nabla g_k(\mathbf{b}')$ ,  $\forall k \in \bigcup_{m=1}^2 \mathcal{P}_m^C$  and  $\nabla h(\mathbf{b}')$  are linearly independent. The gradient of the  $k$ -th inequality constraint is simply the standard unit vector along the  $k$ -th coordinate axis, i.e.,  $\nabla g_k(\mathbf{b}') = \mathbf{e}_j$ . Thus, naturally, the vectors of all active inequality constraints are all linearly independent. The partial derivative of a feasible  $\mathbf{b}'$  satisfying (42) is

$$\frac{\partial h}{\partial b_k} = \begin{cases} \frac{2h_k}{A} (B_{\mathcal{D}_1} + h_k b_k \Delta D) & \text{if } k \in \mathcal{D}_1 \\ -\frac{2h_k}{A} (B_{\mathcal{D}_2} - h_k b_k \Delta D) & \text{if } k \in \mathcal{D}_2 \end{cases}$$

such that

$$\nabla h(\mathbf{b}') = \frac{2}{A(\mathbf{b}')} \left( \sum_{k \in \mathcal{D}_1} h_k (B_{\mathcal{D}_1}(\mathbf{b}') + h_k b'_k \Delta D) \mathbf{e}_k \right) - \frac{2}{A(\mathbf{b}')} \left( \sum_{k \in \mathcal{D}_2} h_k (B_{\mathcal{D}_2}(\mathbf{b}') - h_k b'_k \Delta D) \mathbf{e}_k \right).$$

Note that in general  $\frac{2h_k}{A(\mathbf{b}')} \neq 0, \forall k \in [1 : K]$ , and

$$\begin{aligned} B_{\mathcal{D}_m} + (-1)^{m+1} h_k b'_k \Delta D &\stackrel{(46)}{=} |\mathcal{P}_m| E_{\mathcal{P}_m} + \sqrt{P} h'_m + (-1)^{m+1} h_k b'_k \Delta D \\ &= \begin{cases} E_{\mathcal{P}_m} (|\mathcal{D}_n| - |\mathcal{P}_m^C|) + \sqrt{P} h'_m & \text{if } k \in \mathcal{P}_m \\ |\mathcal{P}_m| E_{\mathcal{P}_m} + \sqrt{P} (h'_m + (-1)^{m+1} h_k \Delta D) & \text{if } k \in \mathcal{P}_m^C \end{cases} \neq 0 \end{aligned}$$

for  $m \neq n$  and  $m \in [1 : 2]$  in case of non-degenerate channel realizations. However, since for

- case c):  $|\bigcup_{m=1}^2 \mathcal{P}_m^C| < K$ ,
- case d):  $|\mathcal{P}_m^C| < |\mathcal{D}_m| < K$ ,

it follows that the span of gradient vectors of active constraints is independent of  $\nabla h(\mathbf{b}')$ . This establishes the LICQ for KKT-points of cases c) and d).<sup>12</sup>

## REFERENCES

- [1] D. Inc., “Data Never Sleeps 7.0,” University of Zurich, Department of Informatics, Tech. Rep., 2019. [Online]. Available: <https://www.domo.com/learn/data-never-sleeps-7>
- [2] “Comprehensive Guide to IoT Statistics You Need to Know in 2020,” <https://www.vxchnge.com/blog/iot-statistics>, accessed: 2020-04-07.
- [3] O. Abari, H. Rahul, and D. Katabi, “Over-the-air Function Computation in Sensor Networks,” *arXiv*, vol. abs/1612.02307, 2016.
- [4] R. C. Buck, “Approximate complexity and functional representation,” *Journal of Mathematical Analysis and Applications*, vol. 70, pp. 280–298, 1979.
- [5] B. Nazer and M. Gastpar, “Computation over multiple-access channels,” *IEEE Transactions on Information Theory*, vol. 53, no. 10, pp. 3498–3516, 2007.
- [6] M. Goldenbaum, H. Boche, and S. Stanczak, “Harnessing Interference for Analog Function Computation in Wireless Sensor Networks,” *IEEE Trans. Signal Processing*, vol. 61, no. 20, pp. 4893–4906, Oct. 2013.
- [7] M. Goldenbaum and S. Stanczak, “Robust Analog Function Computation via Wireless Multiple-Access Channels,” *IEEE Trans. Communications*, vol. 61, no. 9, pp. 3863–3877, 2013.
- [8] B. Nazer and M. Gastpar, “Compute-and-forward: Harnessing interference through structured codes,” *IEEE Transactions on Information Theory*, vol. 57, no. 10, pp. 6463–6486, 2011.
- [9] R. Tandon, Q. Lei, A. G. Dimakis, and N. Karampatziakis, “Gradient Coding: Avoiding Stragglers in Distributed Learning,” in *Proceedings of the 34th International Conference on Machine Learning*, ser. Proceedings of Machine Learning Research, vol. 70, 2017, pp. 3368–3376.

<sup>12</sup>Naturally, the LICQ does not hold for Case b) (all sensors transmit with full power), since the collection of gradient vectors of active constraints spans  $\mathbb{R}^K$ .

- [10] M. M. Amiri and D. Gündüz, “Machine learning at the wireless edge: Distributed stochastic gradient descent over-the-air,” in *2019 IEEE International Symposium on Information Theory (ISIT)*, 2019, pp. 1432–1436.
- [11] F. Molinari, S. Stanczak, and J. Raisch, “Exploiting the Superposition Property of Wireless Communication For Average Consensus Problems in Multi-Agent Systems,” in *2018 European Control Conference*. IEEE, 2018, pp. 1766–1772.
- [12] O. Abari, H. Rahul, D. Katabi, and M. Pant, “Airshare: Distributed coherent transmission made seamless,” in *2015 IEEE Conference on Computer Communications (INFOCOM)*, 2015, pp. 1742–1750.
- [13] M. Goldenbaum and S. Stanczak, “On the channel estimation effort for analog computation over wireless multiple-access channels,” *IEEE Wireless Communications Letters*, vol. 3, no. 3, pp. 261–264, 2014.
- [14] J. Dong, Y. Shi, and Z. Ding, “Blind over-the-air computation and data fusion via provable wirtinger flow,” *IEEE Transactions on Signal Processing*, vol. 68, pp. 1136–1151, 2020.
- [15] X. Cao, G. Zhu, J. Xu, and K. Huang, “Optimal power control for over-the-air computation in fading channels,” *arXiv*, vol. abs/1906.06858, 2019.
- [16] W. Liu and X. Zang, “Over-the-Air Computation Systems: Optimization, Analysis and Scaling Laws,” *arXiv*, vol. abs/1909.00329, 2019.
- [17] G. Zhu and K. Huang, “MIMO Over-the-Air Computation for High-Mobility Multimodal Sensing,” *IEEE Internet of Things Journal*, vol. 6, no. 4, pp. 6089–6103, 2019.
- [18] X. Li, G. Zhu, Y. Gong, and K. Huang, “Wirelessly Powered Data Aggregation for IoT via Over-the-Air Function Computation: Beamforming and Power Control,” *IEEE Transactions on Wireless Communications*, vol. 18, no. 7, pp. 3437–3452, 2019.
- [19] S. P. Boyd and L. Vandenberghe, *Convex Optimization*. Cambridge University Press, 2014.
- [20] S.-P. Han and O. Fujiwara, “An inertia theorem for symmetric matrices and its application to nonlinear programming,” *Linear Algebra and its Applications*, vol. 72, 12 1985.
- [21] R. A. Horn and C. R. Johnson, *Matrix Analysis*, 2nd ed. USA: Cambridge University Press, 2012.